ABSTRACT

Title of Thesis:	DEVELOPMENT OF MODELING AND OPTIMIZATION METHODOLOGIES TO FACILITATE TRANSITION OF HEAT PUMP AND REFRIGERATION SYSTEMS TO LOWER GWP REFRIGERANTS
	Venkata Surya Murali Vijay Preetham Meruva Master of Science, 2025
Thesis Directed By:	Dr. Vikrant C. Aute Research Professor Department of Mechanical Engineering

Abstract: In light of Kigali Amendment, Fluorinated Gas (F-Gas) regulations, and the United States Environmental Protection Agency (EPA) SNAP program calling for the phase out of hydrofluorocarbon (HFC) refrigerants which have an extremely high global warming potential (GWP), it is necessary to transition to lower GWP alternatives. For example, natural refrigerants such as hydrocarbons (HC, e.g., propane (R290), isobutane (R600a), etc.) and carbon dioxide (CO_2) have gained traction as attractive low GWP alternatives for a wide range of residential and commercial heating, ventilation, air-conditioning and refrigeration (HVAC&R) applications which have historically depended on high-GWP refrigerants such as R134a, R410A, R22, and R404A. Moreover, researchers worldwide have also shown immense interest in utilizing refrigerant blends to achieve the required performance whilst minimizing environmental impact. One such area is supermarket refrigeration systems, which often employ multi-stage cascade cycle

configurations due to large temperature lifts, making single-stage vapor compression (VC) systems impractical. A key challenge in this field is selecting environmentally-friendly refrigerants, as many common low-temperature refrigerants have high GWP, high ozone depletion potential (ODP), and/or are flammable. The use of HC refrigerants is also highly regulated due to their flammable nature, hence necessitating high-performance heat exchangers (HXs) with significant size, weight, cost, and refrigerant charge reductions compared to current state-of-the-art to comply with flammable refrigerant charge limits.

Decarbonization of buildings is essential to reducing greenhouse gas emissions, as space and water heating account for a substantial share of energy-related emissions. Transition to heat pump technologies is central to this effort, offering a low-emission alternative to fossil fuel and electric resistance heating. They can substantially reduce greenhouse gas emissions from space and water heating when powered by renewable or low-carbon electricity, making them a key technology for building electrification and climate mitigation goals.

This thesis focuses on the development of modeling and optimization methodologies to facilitate the transition of heat pump and refrigeration systems to lower GWP refrigerants and is applied to three different case studies: (i) refrigerant blend optimization and selection for a supermarket refrigeration system, (ii) a water source heat pump system, and (iii) low-charge air-to-refrigerant HXs for a residential air-conditioning system.

In the first part of the thesis, an approach was developed to design optimal refrigerant blends to serve as lower-GWP alternatives to conventional high-GWP refrigerants while also enhancing system efficiency for a two-stage cascade refrigeration system. Significant improvements in COP by up to 49% and decreases in GWP (< 50) were observed when the optimal blends were incorporated into the system.

In the second part of the thesis, experimental validation of a water source heat pump system model utilizing R32 as the refrigerant and a brazed plate heat exchanger (BPHX) as the condenser was conducted for a steady-state VC system simulation platform to demonstrate the platform's capability to accurately model and simulate VC systems with lower-GWP refrigerants and plate heat exchangers.

In the final part, a comprehensive system-level optimization methodology was developed for air-to-refrigerant tube-fin and finless non-round tube HXs which is capable of designing optimal HX pairs (i.e., condenser and evaporator) with minimal refrigerant charge to replace the baseline HXs in an air-to-R410A air-conditioning system to facilitate the transition to lower GWP refrigerants R32 and R290. System-level simulations with the optimal HX pairs suggest that the optimal HX pairs have comparable thermal-hydraulic performance to the baseline system with significant reduction in HX-level charge (> 70%) , thereby supporting the adoption of lower-GWP natural refrigerants such as R290.

DEVELOPMENT OF MODELING AND OPTIMIZATION METHODOLOGIES TO FACILITATE TRANSITION OF HEAT PUMP AND REFRIGERATION SYSTEMS TO LOWER GWP REFRIGERANTS

by

Venkata Surya Murali Vijay Preetham Meruva

Thesis submitted to the Faculty of the Graduate School of the
University of Maryland, College Park, in partial fulfillment
of the requirements for the degree of
Master of Science
2025

Advisory Committee:

Dr. Vikrant C. Aute, Advisor and Chair
Professor Dr. Bao Yang
Professor Dr. Amir Riaz

Dedication

To my parents - Meruva Venkateswara Rao (father) and Dr. Sunkara Nagamani (mother).

To all my teachers.

Acknowledgements

First and foremost, I would like to take this opportunity to thank and express my sincere gratitude to my advisor Dr. Vikrant Aute, for providing me with the privilege to study at the University of Maryland and engage in the world class research of HVAC&R that is happening at the Center for Environmental Energy Engineering (CEEE). His continued support in my professional and personal life, ensuring growth and comfort at both levels, has been of immense help throughout this journey. I would like to thank Dr. Reinhard Radermacher who guided me in the right way throughout this journey.

I would also like to thank all my professors during my MS, in particular the efforts taken by Dr. Bao Yang and Dr. Amir Riaz to serve on my thesis committee.

I would like to thank Dr. James Tancabel for his continuous assistance, bottom-less pit of patience, attention to detail, guidance, support and especially the discussions we had on the whiteboard, whether it be in his office or on Zoom. He was the perfect mediator between Dr. Vikrant and me. I would also like to thank Dr. Daniel Bacellar for his unmatched professional and personal guidance during my initial days at the university. I am grateful to all my predecessors who worked on VapCyc because without you people, I wouldn't be here. I would also like to thank both present (Leanne Poteet and Beth Panitz) and past (Mary Baugher and Nicole Bradshaw) CEEE program managers and communication coordinators for all their help and support they provide for both myself and CEEE.

I would like to extend a special thank you to all my colleagues and friends at CEEE - Brian O' Malley, my neighbor in the lab, for all the car rides, detailed notes during dry runs, help with my presentations and formatting and discussions on heat exchangers; Suraj Krishnamurti, you were available round-the-clock to help me with coding, everything related to thermodynamics, heat transfer and, numerical methods and part of my work would not have been possible without your assistance in conducting heat exchanger simulations; Alhussain Othman, for engaging me with all the fun and sometimes absurd conversations involving Brian and others and imparting your technical expertise on vapor compression systems to me; Mylena Menezes, for planning all the fun times with our friends and your technical expertise on phase change materials; Arpita Das, for all the banter we shared on cricket and your help with plate heat exchangers; Dr. Haopeng Liu, for your help with technical discussions and code reviews. I would like to thank Tanjebul Alam for his encouragement and emotional support, being a beacon of guidance throughout my journey. I would also like to thank my colleagues at EEHP for all the memories we made throughout my graduate school life. I wish all my colleagues who are working on their research the best of luck in finishing their work.

I would like to thank Roshith Mittakolu, my roommate and friend for his guidance and help from the very beginning in India, to helping me with coursework, technical discussions, selecting our current house, outings, personal and emotional support during my journey here, I will always be indebted to you. I would like to thank my other two support pillars, Vivek Manepalli and Tejaswi Nori, for all the laughter and drama we shared, grocery shopping and car rides. If there ever was a time machine, I would meet you guys six months sooner. I really cherish the times I spent with Veeresh Ayyagari, Ibad Gandikota, Sai Akhilesh Nulu, Saketh Kancheti, Aditya Ramnarayan and my past roommates (Aaryash Raj Sinha, Pratinav Chandra, Sahil Pathan and Krishna Kant Mishra).

I would like to thank my previous mentors during my undergraduate studies in India, professors Nagaraju Dora and Dr. Rajeswara Reddy Resapu for their guidance.

I express my greatest and most profound thanks to my father, Venkateswara Rao Meruva and mother Dr. Sunkara Nagamani for their unwavering encouragement, love, and support in all my endeavors. Watching my mother while she pursued her PhD inspired me to come into the field of research. I would also like to thank all my family members including - Karthik Meruva and his wife Anita for their help, concern, personal support and letting me visit them during my holidays; Prathik Meruva and his wife Ujwala, for the fun conversations and help regarding personal matters and decisions.

Table of Contents

Dedication ii
Acknowledgements iii
Table of Contents vi
List of Tables viii
List of Figures ix
Nomenclature x
Chapter 1: Introduction 1
1.1. Background and Motivation 1
1.2. Literature Review of Cascade Systems and Refrigerant Blends 2
1.3. Literature Review of Lower GWP Systems and Heat Exchanger Optimization 4
Chapter 2: Objectives 8
Chapter 3: Multi-Objective Optimization of Refrigerant Blends for Supermarket Systems 11
3.1. Methodology 11
3.1.1. Two-Stage Cascade System Description 11
3.1.2. Thermodynamic Model Description 12
3.1.3. Estimation of GWP for Refrigerant Blends 13
3.1.4. Model Verification 14
3.2. Problem Formulation 16
3.2.1. Multi-objective Genetic Algorithm (MOGA) 16
3.2.2. Baseline Fluids and Optimization Problem Statement 16
3.2.3. Pure Fluids Selected for Blend Optimization and their GWPs 17
3.3. Results And Discussion 19
3.3.1. Blend Optimization Involving All 30-Fluids 19
3.3.2. Blend Optimization for Only Non-Phased Out Fluids 22
3.4. Conclusions 25
Chapter 4: Brazed Plate Heat Exchanger System Validation 27
4.1. Cycle Description 28
4.2. Solver Description 29
4.3. Validation Results 30
4.4. Conclusions 32
Chapter 5: Comprehensive System-Level Optimization Methodology for the Design of Air-to-Refrigerant HXs for Use of Lower GWP Refrigerants 34
5.1. Cycle Description 35
5.2. Solver Description 36
5.3. HX Component Optimization 36
5.3.1. Multi-Objective Optimization 36
5.3.2. Tube-Fin HXs Optimization Problem Description 36
5.3.3. Tube-Fin HXs Optimization Problem Definition 37
5.3.4. Non-Round Tube HX Design & Optimization Framework 39
5.3.5. Non-Round Tube HX Optimization Problem Description 40
5.3.5.1. Tube Shape Considerations 41
5.3.6. Non-Round Tube HXs Optimization Problem Definition 42
5.4. System-Level Results 42

5.5.Conclusions 46
Chapter 6: Conclusions and Future Work 47
6.1.Summary and Conclusions 47
6.2.Contributions 48
6.3.Future Work 48
6.3.List of Publications 49
Bibliography 50

List of Tables

Table 1. Two-Stage Cascade Refrigeration Cycle Equations 13
Table 2. Calculation of GWP of known refrigerant blends 14
Table 3. Input Parameters and Values Adopted for Verification... 15
Table 4. List of Pure Fluids and GWP-100 Values Used for Optimization [52].......................... 18
Table 5. Min and Max COPs and GWPs During Each Optimization Involving All 30-fluids..... 20
Table 6. Refrigerant Blend Compositions for an Optimization Case Involving All 30-fluids..... 22
Table 7. Min and Max COPs and GWPs During Each Optimization Involving Only Non-Phased Out Fluids... 23
Table 8. Refrigerant Blend Composition for a Non-Phased Out Fluid Optimization Case.......... 24
Table 9. Absolute Error Statistics 32
Table 10. MOGA settings 36
Table 11. TFHX Thermal-Hydraulic Performance Correlations 37
Table 12. Design Space for TFHXs 38
Table 13. NTHX Thermal-Hydraulic Performance Correlations 41

List of Figures

Figure 1. Schematic of a Two-Stage Cascade Refrigeration System 12
Figure 2. Model Verification using Simulation Data from [7] 15
Figure 3. COP vs GWP for Blend Optimization Involving All 30-fluids 20
Figure 4. COP vs GWP for Blend Optimization Involving Only Non-Phased Out Fluids (21 total fluids) 24
Figure 5. BPHX Cycle Schematic 29
Figure 6. Simulated vs Experimental Capacity Normalized.. 30
Figure 7. Simulated vs Experimental Power Normalized.. 31
Figure 8. Simulated vs Experimental Mass Flow Rate Normalized... 31
Figure 9. Baseline Cycle Schematic 35
Figure 10. HX Optimization Framework [42] 40
Figure 11. Schematic of (left) HX with Shape-Optimized Tubes; (right) Generic Tube-Fin Condenser 41
Figure 12. Sample NURBS shapes 41
Figure 13. System-Level Metrics with Optimal HXs Compared to Baseline System HXs 43
Figure 14. Charge Comparison Between Optimal HXs and Baseline HXs................................. 44
Figure 15. Internal Volume Comparison Between Optimal HXs and Baseline HXs.................. 44

Nomenclature

A	Heat transfer area	(m^2)
AC	Air-conditioning	(-)
A_f	Face area	(m^2)
APE	Absolute percentage error	(%)
BL	Baseline	(-)
BPHX	Brazed plate heat exchanger	(-)
C	Condenser/Condensing	(-)
CFC	Chrlorofluorocarbons	(-)
CHX	Cascade heat exchanger	(-)
COP	Coefficient of performance	(-)
E	Evaporater/Evaporating	(-)
FPI	Fins per inch	(-)
GWP	Global warming potential	(-)
h	Enthalpy	J/kg
HC	Hydrocarbon	(-)
HFO	Hydrofluorocarbon	(-)
HTC	High temperature cycle/heat transfer coefficienct	(-)/$Wm^{-2}K^{-1}$
HX	Heat exchanger	(-)
H_{HX}	Heat exchanger length	(m)
is	Isentropic	(-)
LTC	Low temperature cycle	(-)
L_{HX}	Heat exchanger length	(-)

MF	Mass fraction	(-)
NTHX	Non-round tube heat exchanger	(-)
ODP	Ozone depletion potential	(-)
P	Pressure	(Pa)
PHX	Plate heat exchanger	(-)
ref	Refrigerant	(-)
SHR	Sensible heat ratio	(-)
T	Temperature	K/°C
TFHX	Tube-fin heat exchanger	(-)
VC	Vapor compression	(-)
V_{HX}	Heat exchanger envelope volume	(m^3)
ΔP	Pressure drop	(Pa)
$\dot{Q}$	Capacity	(W)
η	Efficiency	(-)
$\dot{m}$	Mass flow rate	kg/s
β	Metric of interest	(-)

Chapter 1: Introduction

1.1.Background and Motivation

A vapor compression system is a thermodynamic cycle employed to transfer heat from a region of low temperature to high temperature. This technology is the backbone of heating, ventilation, air-conditioning, and refrigeration (HVAC&R) systems and supports a wide range of applications that include indoor climate control for human comfort, food preservation, and industrial cooling. While these systems are essential to the modern infrastructure, they are major energy consumers and contribute substantially to global greenhouse gas emissions due to the use of high-GWP refrigerants, thereby posing challenges related to both energy sustainability and environmental impact. According to U.S. Energy Information Administration (EIA), residential and commercial sectors consumed 28% of the total energy consumption in 2023 [1]. Air-conditioning is one of the largest uses of electricity in U.S. residential and commercial buildings accounting for 19% and 14% of total electricity consumption respectively with an additional 18% consumed for ventilation [2]. Similarly, space heating accounted for 42% of energy consumption in the residential sector with increasing costs [3].

Therefore, reducing the energy consumption along with global warming impact of HVAC&R systems is going to be very crucial. This can be done by utilizing (i) advanced system configurations such as vapor injection cycles, cascade cycles etc. (ii) high performance next generation heat exchangers (HX) as HXs are critical components in a vapor compression system and can directly play a role in global energy sustainability and (iii) use of environmentally friendly refrigerants such as lower-GWP refrigerants, blends and/or natural refrigerants. Also, steady state vapor compression system simulation and optimization will be crucial in assessing the effectiveness and environmental impact associated with the above options.

1.2.Literature Review of Cascade Systems and Refrigerant Blends

In supermarkets, low-temperature refrigeration keeps meats, vegetables, and dairy products frozen and fresh, requiring evaporating temperatures in the range of -30°C to -50°C. For this application, cascade systems are suitable [4], employing multiple refrigeration cycles to achieve extremely low temperatures for applications requiring precise and efficient temperature control. In two-stage cascade refrigeration systems, two single-stage vapor compression systems are thermally coupled through a cascade HX. Such cycles are beneficial to use for high temperature lift applications.

In the early days, refrigerants such as R11, R12, R13, R22, R500, and R502 were widely used in cascade refrigeration systems [5]. Due to environmental challenges related to global warming and ozone layer depletion resulting from using these refrigerants, natural and lower Global Warming Potential (GWP) refrigerants such as CO_2 and NH_3 gained popularity as working fluids for two-stage cascade systems. A thermodynamic analysis of a two-stage cascade system with CO_2 for the low-temperature cycle and NH_3 for the high temperature cycle was performed by [4] to optimize the parameters- condensing and evaporating temperatures, subcooling, superheating, and cascade temperature difference. Correlations were developed for maximum COP, optimum evaporating temperature for NH_3, and optimum mass flow ratio which are functions of the above-mentioned parameters with reported COPs between 1.2-1.5. Similar analyses were conducted by [6] and [7] to determine optimum condensing temperature and maximum COP. This was followed up with an experimental evaluation of a prototype 9 kW system with CO_2 and NH_3 as the refrigerants varying CO_2 evaporating and condensing temperatures by [8] and verified the optimum CO2 condensing temperature they obtained with the findings from [6] and [7] .Due to challenges posed with using

CO_2 and NH_3 [5], researchers began focusing their efforts on other low GWP refrigerants and their blends. Thermodynamic analysis of a two-stage cascade system with R170 and R290 refrigerants was conducted by [9], achieving COPs from 1.1-1.8 and compared the performance of the system when using R22 and R23. [10] utilized R23, R41, and R170 for the LTC with R32, R1234yf, R1234ze, R161, R1270, R290, and R717 for the HTC in a thermodynamic energy and exergy analysis of a two-stage cascade system and reported COPs between 0.6-2. [11] performed a detailed literature and thermodynamic study on a two-stage cascade system using R41 as the LTC refrigerant and R1234yf, R423A, R601, R601A, R1233zd(E), and R170 as HTC refrigerants to evaluate low-GWP refrigerant pairs and the impact of various operating parameters on system performance.

In addition to the previously mentioned use of lower-GWP refrigerants, researchers worldwide have shown an immense interest in making and using refrigerant blends or mixtures. Refrigerant blends which comprise of two or more pure substances, are engineered to optimize thermodynamic properties, improve energy efficiency of the system, and reduce flammability, toxicity and GWP in comparison to traditional single-component refrigerants [12]. Another impetus for utilizing refrigerant blends is the ability to tailor temperature glide, pressure levels, and enthalpy of vaporization to better match the HX design and characteristics allowing for better temperature matching between the refrigerant and the secondary fluid, thus enhancing heat transfer efficiency and improving COP for different system operating conditions and applications [13]. Refrigerant blends can also enable retrofit applications, allowing present systems to transition from high-GWP refrigerants such as R410A or R404A to more environmentally acceptable alternatives without substantial hardware alterations [14]. Also, hydrocarbons that have low GWP and possess good thermophysical characteristics, such as R170, R1270, R600a, and R290, may not seem to be attractive as single-component refrigerants due to their high flammability but may be considered as blend components. So, as refrigerant blends started gaining popularity, [15] performed a thermodynamic parametric analysis of a two-stage cascade system varying CO_2 mass fraction for blends CO_2/R1270, CO2/NH_3, and CO_2/R170 in both stages and reported COPs between 1.64-2.34. [16] conducted a theoretical screening analysis to evaluate low-GWP and mildly flammable mixtures as alternatives for R410A for a single-stage heat pump system where the blends consist of up to five components chosen from a list of 12 pure fluids. Multi-parameter optimization was done to achieve GWP < 150, mild flammability, and maximum COP.

1.3.Literature Review of Lower GWP Systems and Heat Exchanger Optimization

Air-to-refrigerant HXs are fundamental components in heating, ventilation, air-conditioning, and refrigeration (HVAC&R) systems, serving as the main heat transfer component(s). The Kigali Amendment [17] has called for the phase out of HFCs which have an extremely high global warming potential (GWP) and this has resulted in the HVAC&R industry shifting focus to systems utilizing natural working fluids. The fluorinated gas (F-Gas) regulations of the European Union [18] has prohibited the use of high GWP gases since 2023. Therefore, it is necessary to move towards lower GWP alternatives. Use of hydrofluoro-olefins (HFOs) as low GWP alternatives have environmental concerns since they are per and poly-fluoroalkyl substances (PFAS) which can degrade to trifluoroacetic acid (TFA) which has an extremely high environmental stability. Hence, natural refrigerants such as carbon dioxide, ammonia and hydrocarbons are being considered as low GWP alternatives.

Among hydrocarbons, propane (R290) with GWP < 1 has received a considerable amount of interest due to superior thermophysical properties and can enable smaller components and thus lower refrigerant charge compared to current refrigerants such as R134a and R410A [19].

However, R290 is highly flammable (ASHRAE Class A3), and thus the refrigerant charge quantity in systems is highly regulated. Thus, reducing system refrigerant charge is a key consideration for designing next-generation HVAC&R systems with R290. The ISO 5149 [20] and IEC 60335 [21] standards are the primary international standards responsible for setting refrigerant charge limits on HVAC equipment. Most local standards around the world are based on these standards and may have minor modifications. For example, the EN 60335-2-89 [22] standard and the UL 60335-2-89 [23] standards are based on the IEC 60335-2-89 [24] standard for commercial equipment and ice-makers. The IEC 60335-2-24 [25] standards allow a charge limit of 150g for domestic refrigerating appliances. However, for commercial systems, the IEC 60335-2-89 standard increased the charge limit from 150g to 494g for A3 refrigerants and to 1.2 kg for A2L refrigerants. The ISO standard 5149 [26] prescribes a maximum charge limit of 1 kg for R290, with an 80% reduction in charge limit for locations meant for public. With these strict charge limits, designing systems with R290 must also account for system charge.

The feasibility of hydrocarbon (HC) natural refrigerants and their mixtures to replace hydrofluorocarbons (HFC) and hydrochlorofluorocarbons (HCFC) has been well-studied across the literature. [27] is one of the papers which discussed the possibility of replacing existing manmade refrigerants (in their case R12) with flammable refrigerant mixture of R290/R600a. From then on, many studies were performed to investigate the feasibility of substituting existing refrigerants with hydrocarbons by [28], [29], [30], [31]. The most common candidates were either R290, R600a or a mixture of these two refrigerants. It has been shown that hydrocarbons have a slightly better thermo-hydraulic performance compared to existing alternatives and are also compatible with POE oils [31]. Recently, the LC 150 project [32] focused on brine-water secondary loop systems, to reduce the charge of R290 in the system. They were able to bring down the specific charge down to 10 g/kW, with a system which provided 12.8 kW of heating with 124g of R290. [33] studied air-conditioning and heat pump systems and found that HCs and their mixtures represent the best balance between COP and volumetric capacity. [34] experimentally evaluated R134a, R290, R404A, R407C, and R410A as potential substitutes for R22 in HVAC&R systems and found R290 to be a good long-term replacement, with a reported COP of up to 3.55. Experimental testing of an R290 system with aluminum microchannel HXs conducted by [35] resulted in system charges between 140-300 grams and COPs ranging from 2.5-5 depending on the evaporating temperature. [36] numerically investigated the impact of capillary lengths and microchannel condenser port diameters to obtain the optimum charge for a split packaged air-conditioner. The authors conducted drop-in testing using the optimized R290 charge and observed reduced capacity and higher EER compared to R22, thus recommending a HX redesign for safe and efficient system operation. [37] conducted drop-in testing of R290 as a substitute for R410A for a split air-conditioner and observed that the R290 system (170 g) utilized two times less charge compared to the R410A system (340 g).

In an air source heat pump, the condenser and evaporator have a much higher thermal resistance on the air side, which results in a loss of cycle capacity and increased power consumption. Therefore, optimization of these HXs is important for high efficiency heat pumps. A lot of work has been done on the optimization of HXs, and a comprehensive review was done by [38]. As noted above, many researchers found that one of the keys to reducing refrigerant charge was to redesign the HXs. In this context, reducing refrigerant charge is often associated with minimizing the HX internal volume [39], i.e., utilizing compact HXs with small characteristic diameters (≤6.0 mm, [40]) whose high heat transfer area-to-volume ratio can yield significant HX size, and thus charge, reductions. However, compact HXs require fins to achieve the required capacity, resulting in increased airside pressure drop, material consumption, and fouling/frosting potential. Advancements in computational fluid dynamics (CFD), finite element analysis (FEA), optimization algorithms, and manufacturing capabilities have allowed researchers to innovate HX design practices and apply primary heat transfer surface optimization to achieve highly compact HXs that do not require fins. To this end, [41] developed a multi-scale analysis and shape and topology optimization framework for novel non-round, small-diameter tubes which was experimentally validated using an additively manufactured proof-of-concept design. This framework was improved by [42] to include multi-physics analyses including tube mechanical strength, enabling further tube size, material, and charge reductions without compromising tube structural integrity and was utilized to optimize air-to-natural-working-fluid HXs for R290 condensers [43] and later supercritical CO_2 gas coolers [42], showing significant promise for HXs based on non-round tubes for use with low-GWP refrigerants.

Chapter 2: Objectives

This focus of this thesis on the development of modeling and optimization methodologies to facilitate the transition to lower GWP refrigerants for heat pump and refrigeration systems and is applied to three different case studies: (i) refrigerant blend optimization and selection for a supermarket refrigeration system, (ii) a water source heat pump system, and (iii) low-charge air-to-refrigerant HXs for a residential air-conditioning system.

(i) In the third chapter, a two-stage cascade system was thermodynamically modeled and verified using operating conditions and refrigerants from literature. Next, refrigerant blend optimization was conducted using Multi-Objective Genetic Algorithm (MOGA) to determine optimal refrigerant blend compositions for both low temperature cycle (LTC) and high temperature cycle (HTC) to maximize COP and minimize GWP. The identified research gap lies in the absence of comprehensive studies that utilize a wide range of refrigerants—specifically 30 candidate fluids—to develop optimal refrigerant blends for both the high-temperature and low-temperature cycles of a two-stage cascade refrigeration system, aiming to reduce GWP and maximize COP. Initially 15 pure fluids were considered for blend composition for both the LTC and HTC. Fluids with negligible mass fractions were removed from the blend, and the remaining fluids were utilized to further optimize the blend until five or fewer component fluids remained for both the LTC and HTC. The optimization procedure was repeated for fluids which have not yet been phased out by the U.S. EPA [44]. The optimal refrigerant blends were compared to determine the impact of blend composition on system performance and GWP and also to the baseline systems with one refrigerant per fluid loop.

(ii) In the fourth chapter, a brazed plate heat exchanger (BHPX) was modeled using an in-house PHX simulation platform ([45] and [46]) that can effectively capture the thermal-hydraulic behavior of BPHXs. Next, a water source heat pump using lower-GWP R32 as the refrigerant and containing the BPHX and an air-to-refrigerant HX is validated against independent laboratory experimental data using a steady-state vapor compression system simulation platform ([47], [48], [49]) to demonstrate the platform's capability to accurately model and simulate VC systems with lower-GWP refrigerants and plate heat exchangers.

(iii) In the fifth chapter, a comprehensive system-level optimization methodology was developed for air-to-refrigerant tube-fin and finless non-round tube HXs which can design optimal HX pairs (i.e., condenser and evaporator) with minimal refrigerant charge to replace the baseline HXs in an air-to-R410A air-conditioning system. Tube-fin HXs with louver fins for the condenser and slit fins for the evaporator are first optimized using this methodology to design low charge air-to-refrigerant HXs with the refrigerants being R410A, R32 and R290. Next, an HX optimization framework for novel shape-optimized, non-round tubes [42] combined with the optimization methodology is applied to design R290-based condensers and evaporators with conventionally-manufacturable, non-round tubes. The baseline system is the air-to-R410A air-conditioning (AC) system which utilizes a tube-fin condenser and evaporator [50]. The optimal HXs are designed to deliver the same or better thermal-hydraulic performance compared to the baseline R410A HXs while also significantly reducing the refrigerant charge. The identified research gap pertains to the lack of comprehensive evaluation of geometry- and circuitry-optimized HXs—specifically those employing louvered and slit fins, as well as non-round tube configurations—within a full system environment. The system performance using both the baseline (R410A) and optimal tube-fin and non-round tube HXs was calculated using the aforementioned system steady-state simulation platform to assess the potential of R32 and R290 as an R410A replacement for air-conditioning applications. The results of this study will provide critical insights into the viability and advantages of using R32 and R290 in residential air-conditioning applications to help facilitate the adoption of flammable and mildly-flammable refrigerants worldwide.

Chapter 3: Multi-Objective Optimization of Refrigerant Blends for Supermarket Systems

Multi-stage cascade cycles are often utilized for applications such as supermarket refrigeration where a single vapor compression cycle is impractical for large temperature lifts. Along with low COPs, refrigerants selection for these systems is one of the main challenges in this field, especially since many common low-temperature refrigerants have large environmental impacts, e.g., GWP, ozone depletion potential (ODP), and/or flammability. To overcome this, researchers have proposed refrigerant blend optimization, targeting fluids that deliver high system efficiency with minimal overall environmental impact. In this section, a thermodynamic analysis-based multi-objective optimization approach was conducted to design refrigerant blends for supermarket two-stage cascade systems. The benefits of the proposed refrigerant blends are discussed in detail to gain insights into potential future refrigerants for low temperature refrigeration. The proposed approach can enable future design of novel refrigerant blends for multi-cascade refrigeration systems with improved efficiencies while also satisfying GWP constraints.

3.1.Methodology

3.1.1.Two-Stage Cascade System Description

Figure 1 depicts the two-stage cascade refrigeration system, which consists of two distinct, four-component refrigeration circuits which use an appropriate refrigerant for the required temperature range and are thermally connected through a cascade heat exchanger.

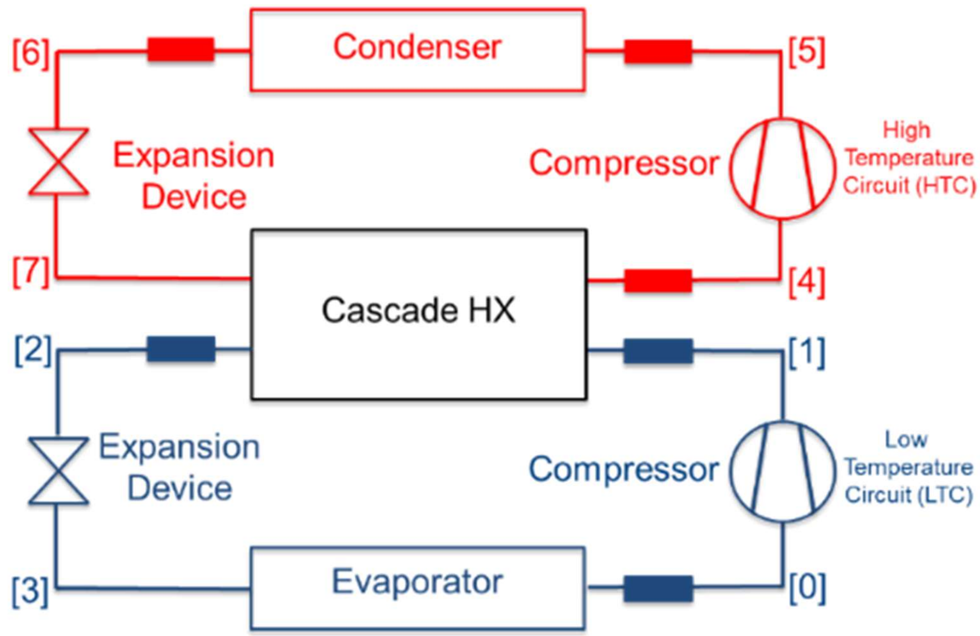

Figure 1. Schematic of a Two-Stage Cascade Refrigeration System

The following assumptions are made during the analysis:

1. All processes are steady-state, steady-flow processes.
2. The changes in kinetic and potential energy are negligible.
3. All expansion processes are isenthalpic, and all compression processes are isentropic.
4. Heat losses and pressure drops in the linking pipes and HXs have been neglected

3.1.2.Thermodynamic Model Description

The two-stage cascade refrigeration system was modelled using the equations listed in Table 1.

Table 1. Two-Stage Cascade Refrigeration Cycle Equations

Parameter	Equation
LTC Evaporator Capacity	$\dot{Q}_{LTC} = \dot{m}_{LTC}(h_0 - h_3)$
LTC Compressor Power Consumption	$\dot{W}_{LTC} = \frac{\dot{m}_{LTC}(h_{1\text{is}} - h_0)}{\eta_{is\_LTC}}$
HTC Compressor Power Consumption	$\dot{W}_{\text{HTC}} = \frac{\dot{m}_{HTC}(h_{5s} - h_4)}{\eta_{is\_\text{HTC}}}$
Cascade HX Capacity	$\dot{Q}_{CHX} = \dot{m}_{LTC}(h_1 - h_2) = \dot{m}_{HTC}(h_4 - \text{h}_7)$
HTC Condenser Capacity	$\dot{Q}_C = \dot{m}_{HTC}(h_5 - h_6)$
Overall System COP	$COP = \frac{\dot{Q}_{LTC}}{\dot{W}_{\text{HTC}} + \dot{W}_{\text{LTC}}}$
System Carnot COP	$COP_{carnot} = \frac{T_{E,LTC}}{T_{C,HTC} - T_{E,LTC}}$

3.1.3.Estimation of GWP for Refrigerant Blends

The GWP of a blend is typically estimated using a mass-weighted average approach (Eq. (1)) as recommended by [51] and [16]:

$$GWP = \sum_{1}^{n} MF_{pure,i} GWP_{pure,i} \qquad \text{Eq. (1)}$$

where $MF_{pure,i}$ is the component mass fraction and $GWP_{pure,i}$ is the component GWP as given by the IPCC AR6 report [52]. The total cascade system GWP is defined as the sum of the GWPs of the LTC and HTC refrigerants. Equation 1 was verified by comparing the calculated GWP of known refrigerant blends with their reference values [53] (Table 2). The calculated GWPs matched well with the reference values, and the maximum percentage difference was 6.35% for R440A.

Table 2. Calculation of GWP of known refrigerant blends

Refrigerant	Calculated GWP (Eq. (1))	Reference GWP [53]	Percentage Difference
R410A	2255	2285	-1.31%
R454A	270	263	+2.66%
R454B	531	516	+2.90%
R404A	4728	4808	-1.66%
R470A	1057	1064	-0.65%
R428A	4060	4141	-1.95%
R440A	184	173	+6.35%
R465A	162	158	-2.53%

3.1.4.Model Verification

The two-stage cascade system model was verified against simulation data from [7] for the operating conditions and refrigerants listed in Table 3. The cycle considers no subcooling, superheat, pressure drop or heat loss for any component. Thermodynamic property calculations utilized NIST REFPROP [54] augmented with curve-fits described in [55]. The predicted COP is compared to the COP from [7] in Figure 2 for different cascade condensing temperatures. The present model shows good agreement with previous work, with a maximum deviation of 1.7%.

Table 3. Input Parameters and Values Adopted for Verification

Parameter	Input Value
LTC Refrigerant	CO_2
HTC Refrigerant	NH_3
Cooling Capacity	175 kW
LTC T_E	-50°C
Cascade T_E	-25.64°C to -3.7°C
HTC T_C	35°C
Cascade HX Temperature Difference	5°C
LTC and HTC Compressor η_{is}	[7]

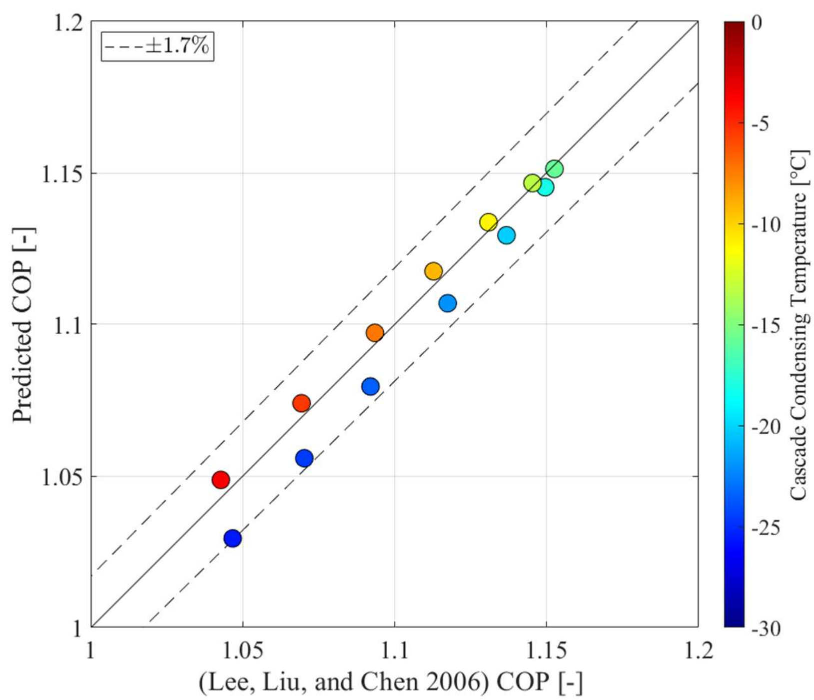

Figure 2. Model Verification using Simulation Data from [7]

3.2.Problem Formulation

3.2.1.Multi-objective Genetic Algorithm (MOGA)

The optimization of refrigerant blends is conducted using MOGA [58] which is a type of evolutionary algorithm designed to solve optimization problems involving multiple and often conflicting objectives. This differs from single-objective methods that find one optimal solution where MOGA aims to identify a set of trade-off solutions known as Pareto-optimal front, where no objective can be improved without degrading another. A population-based approach is utilized where a diverse group of candidate solutions evolve over generations through operators like selection, crossover, mutation, and elitism. One of the key features of MOGA is its ability to maintain and improve a diverse set of non-dominated solutions in each generation that allows for an effective approximation of the Pareto front. Popular algorithms like NSGA-II [58] incorporate mechanisms to ensure elitism and diversity, ensuring convergence and broad coverage of trade-off solutions.

3.2.2.Baseline Fluids and Optimization Problem Statement

The cycle parameters for the blend optimization are given in Table 3, except that the compressor isentropic efficiencies are set to 0.65 and cascade condensing temperature is set to -15.76°C. The baseline cases assume the following refrigerant combinations (LTC/HTC): (i) CO_2/NH_3 [7], (ii) R170/R32 [10], (iii) R23/R152a [56] and (iv) R13/R12 [57]. Optimization is conducted using a MOGA [58] with 500 total iterations, population size of 200, and population replacement of 10%. The optimization problem statement is shown in Eq. (2).

$$
\begin{gathered}
Max\,COP; Min\,GWP \\
s.t. \\
1a.\ Atmost\,15\ fluids\,on\,LTC\ and\ HTC\ are\,optimized \\
1b.\,Filter\,1a.\,fluids\ with\,MF \le 0.5\%\ and\ run\,again \\
1c.\,Filter\,1b.\,fluids\ with\,MF \le 0.5\%\ and\ run\,until \\
five\,or\ fewer\ fluids\,remain\,each\,on\,LTC\ and\ HTC\ side
\end{gathered}
\qquad \text{Eq. (2)}
$$

The overall objective is to identify refrigerant blend couples which maximize system COP and minimize system GWP (sum of GWPs of LTC and HTC blends) for the cascade system of interest. In the first optimization problem (1a), 15 refrigerants are considered for both the LTC and HTC to create two blends. The middle point of the Pareto set is used as the basis for the second optimization problem (1b), where the component fluids with mass fraction less than or equal to 0.5% are removed since their presence has minimal impact on performance. The remaining fluids are filtered and optimized until five or fewer fluids remain on each side with each fluid having considerable mass fraction. The same optimization procedure was then repeated, beginning with refrigerants which have not yet been phased out by the US EPA [44].

3.2.3.Pure Fluids Selected for Blend Optimization and their GWPs

The 30 candidate fluids selected for blend optimization are listed in Table 4 and are taken and categorized from [10] and [11].

Table 4. List of Pure Fluids and GWP-100 Values Used for Optimization [52]

LTC		HTC	
Fluid	GWP	Fluid	GWP
CO_2	1	R600	0.006
R1233zd(E)	3.88	R290	0.02
R41	135	R170	0.437
R124*	597	R1234yf	0.501
R245fa	962	R1234ze(E)	1.37
R236ea	1500	R1270	1.8
R134a	1530	R600a	3
R125	3740	R123*	90.4
R143a	5810	R152a	164
R113*	6520	R32	771
R236fa	8690	R141b*	860
R115*	9600	R22*	1960
R116	12400	R142b*	2300
R23	14600	R227ea	3600
R13*	16200	R12*	12500

*Phased out refrigerant [44].

3.3.Results And Discussion

3.3.1.Blend Optimization Involving All 30-Fluids

The COP and GWP of baseline cases and results of the 30-fluids optimization are shown in Figure 3. The range of COP and GWP achieved while all 30-fluids participated is shown in Table 5 along with the percentage of Carnot COP. The maximum COP achieved is 1.52, which is 32% better than the baseline CO_2/NH_3 case. However, the GWP values are in between 535 and 759 whereas CO_2/NH_3 case has a GWP of 1. When compared to the next lowest GWP from baseline cases (R170/R32), the minimum COP achieved by the 30-fluids case is 34% better with 30% lower GWP. The middle point of the 30-fluids case (COP = 1.46, GWP = 623) is highlighted with a red circle in Figure 3, and the detailed results are summarized in Table 6. Note that the fluids with mass fractions less than 0.5% correspond to those fluids with some of the highest GWPs, and targeting minimum GWP would result in blends with minimal amounts of these fluids.

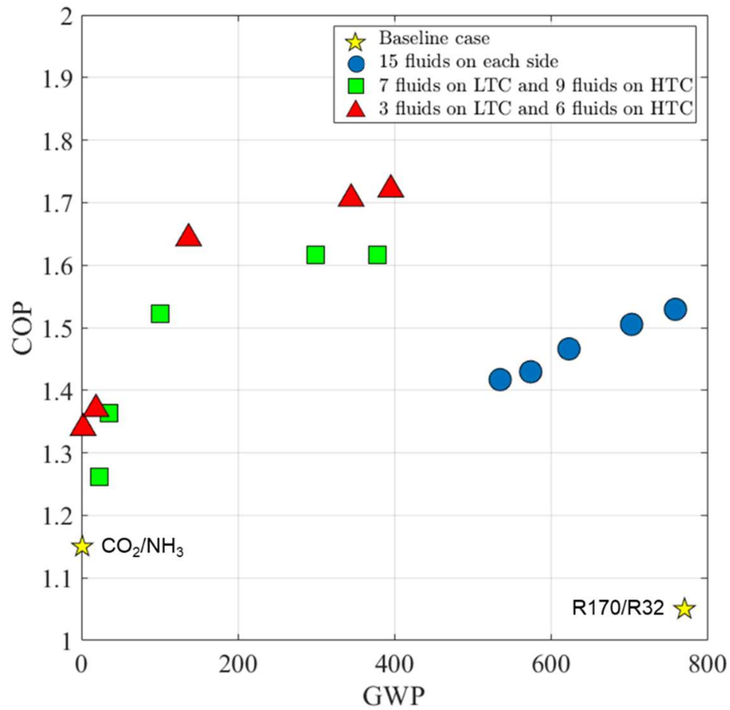

Figure 3. COP vs GWP for Blend Optimization Involving All 30-fluids

Table 5. Min and Max COPs and GWPs During Each Optimization Involving All 30-fluids

Fluids	Min COP	% of Carnot COP	Max COP	% of Carnot COP	Min GWP	Max GWP
30	1.41	53.81	1.52	58.01	535	759
16	1.26	48.09	1.61	61.45	22	378
9	1.33	50.76	1.72	65.64	2	395

The low mass fraction refrigerants were then filtered out, leaving 16-fluids (7 LTC fluids, 9 HTC fluids) for Case 1b. The maximum COP (Figure 3, Table 5) achieved by the 16-fluids case is 1.61, which is 40% higher than the baseline CO_2/NH_3 case and 5% better than the maximum COP achieved by 30-fluids case. GWP values for this case range from 22-378, which is significantly lower than with the 30-fluids case. The minimum COP of 1.26 is 20% better than the R170/R32 case with 97% lower GWP. The middle point of the 16-fluids case (COP = 1.52, GWP = 100) is highlighted with a red circle in Figure 3, and detailed results are shown in Table 6. CO_2 and R1233zd(E), which are the two lowest GWP fluids on the LTC, emerged as the dominant fluids occupying 47% and 51.8% whereas on the side of HTC, R1234ze(E) and R123 are the dominant fluids with 40.3% and 40.7%, significantly reducing the GWP compared to the 30-fluids case while also achieving higher COPs. Once again, refrigerants with the highest GWPs appeared in the lowest concentrations in order to minimize GWP.

The low concentration fluids were again filtered, leaving 9-fluids (3 LTC fluids, 6 HTC fluids) for Case 1c. The 9-fluids case produced a maximum COP of 1.72, which is 49% better than the baseline CO_2/NH_3 case, 6% better than the maximum COP achieved by 16-fluids case, and 13% better than the maximum COP achieved by 30-fluids case with GWP values ranging from 2-395 (Table 5, Figure 3). A minimum GWP value of 2 with a corresponding COP of 1.33 is achieved, which is 15% higher than the baseline CO_2/NH_3 case. The middle point of the 9-fluids case (COP = 1.64, GWP = 136) is highlighted with red circle in Figure 3 and detailed results are shown in Table 6. CO_2 emerged as the dominant fluid (99.7%) for the LTC, whereas R123 emerged as the dominant fluid (66.6%) for the HTC.

Table 6. Refrigerant Blend Compositions for an Optimization Case Involving All 30-fluids

30-fluids (MF in %)	LTC: R115 (0.17) / R13 (0.23) / R125 (1.38) / R41 (21.8)/ R23 (0.08) / CO_2 (24.5) / R236ea (4.92) / R124 (14.2) / R143a (0.16) / R116 (0.11) / R1233zd(E) (24.2) / R134a (0.5) / R113 (0.39) / R236fa (0.02) / R245fa (7.14)
	HTC: R1270 (0.29) / R12 (0.04) / R22 (0.13) / R32 (0.40) / R152a (1.18) / R227ea (0.33) / R600a (5.27) / R170 (4.38) / R290 (0.81) / R1234yf (9.57) / R1234ze(E) (31.1) / R600 (0.71) / R141b (15.6) / R142b (0.16) / R123 (29.9)
16-fluids (MF in %)	LTC: R125 (0.01) / R41 (0.18) / CO_2 (47.0) / R236ea (0.01) / R124 (0.20) / R1233zd(E) (51.8) / R245fa (0.68)
	HTC: R152a (0.05) / R600a (0.59) / R170 (4.26) / R290 (1.11) / R1234yf (0.33) / R1234ze(E) (40.3) / R600 (6.46) / R141b (6.07) / R123 (40.7)
9-fluids (MF in %)	LTC: CO_2 (99.7) / R1233zd(E) (0.24) / R245fa (0.01)
	HTC: R170 (2.43) / R290 (5.28) / R1234ze(E) (16.1) / R600 (0.78) / R141b (8.78) / R123 (66.6)

3.3.2.Blend Optimization for Only Non-Phased Out Fluids

An additional optimization study was conducted using the same procedure above, but all fluids that are (or will be) phased out according to the US EPA [44] were removed. This resulted in 11-LTC fluids and 10-HTC fluids for optimization Case 1a. The results of the optimization are shown in Figure 4, and the range of COPs and GWPs achieved during the 21-fluids case is shown in Table 7. The maximum COP achieved is 1.44, which is 25% better than the baseline CO_2/NH_3 case and 10% and 5% lower than the 16-fluids and 30-fluids cases, respectively. Also, GWPs range from 64-135, which are significantly lower compared to the 30-fluids and 16-fluids cases. This is a direct result of not including the phased-out fluids, which largely have very high GWP. The middle point of the 21-fluids case (COP = 1.43, GWP = 95) is highlighted with a red circle in Figure 4 and detailed results are shown in Table 8. CO_2 and R1233zd(E) emerged as dominant fluids with 40.1 and 38.8%, like the 16-fluids case. R600 is the dominant fluid on the HTC, whereas R1234ze(E) and R123 (phased out) were dominant in the 16-fluids case on the HTC. Moreover, R125 / R23 / R236ea / R143a / R116 / R134a / R236fa had mass fractions less than 0.5% on the LTC whereas R1270 / R227ea / R290 / R1234yf / R1234ze(E) did so on the HTC. These refrigerants were filtered, leaving with 9-fluids (4 LTC fluids, 5 HTC fluids) for the next optimization.

Table 7. Min and Max COPs and GWPs During Each Optimization Involving Only Non-Phased Out Fluids

Fluids	Min COP	% of Carnot COP	Max COP	% of Carnot COP	Min GWP	Max GWP
21	1.37	52.29	1.44	54.96	64	135
9	1.41	53.81	1.52	58.01	2	70

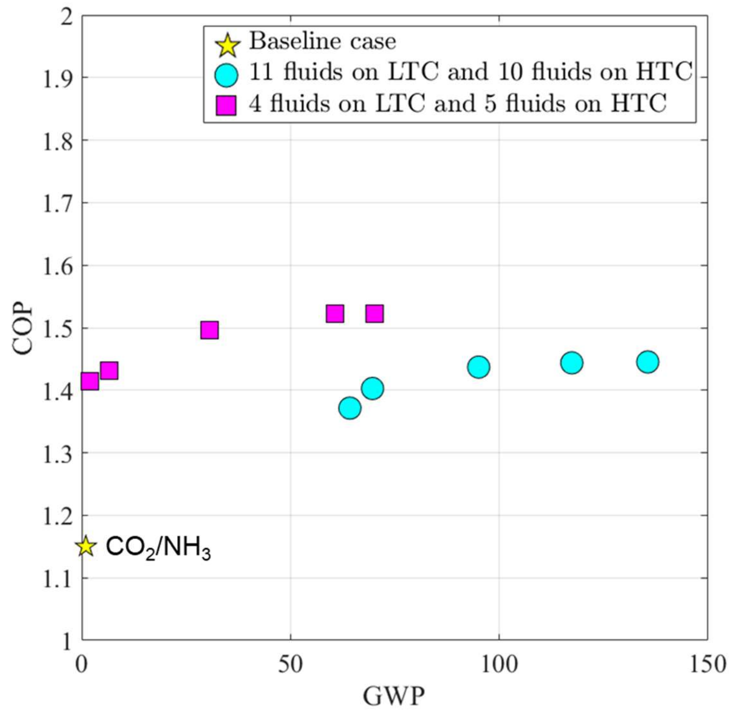

Figure 4. COP vs GWP for Blend Optimization Involving Only Non-Phased Out Fluids (21 total fluids)

Table 8. Refrigerant Blend Composition for a Non-Phased Out Fluid Optimization Case

21-fluids (MF in %)	LTC: R125 (0.01) / R41 (19.2)/ R23 (0.02) / CO_2 (40.1) / R236ea (0.53) / R143a (0.04) / R116 (0.03) / R1233zd(E) (38.8) / R134a (0.02) / R236fa (0.07) / R245fa (1.11)
	HTC: R1270 (0.23) / R32 (3.73) / R152a (0.68) / R227ea (0.07) / R600a (3.37) / R170 (11.4) / R290 (0.31) / R1234yf (0.01) / R1234ze(E) (0.10) / R600 (80.0)
9-fluids (MF in %)	LTC: R41 (0.18) / CO_2 (47.0) / R1233zd(E) (51.8) / R245fa (0.68)
	HTC: R32 (3.80) / R152a (0.01) / R600a (0.08) / R170 (8.14) / R600 (87.9)

The maximum COP achieved during the 9-fluids case is 1.52 which is 32% higher than the baseline CO_2/NH_3 case. This is the same COP achieved by the 30-fluids case, but the maximum GWP (70) is now 90% lower. A minimum GWP of 2 was observed during this case with a corresponding COP of 1.41, which is 22% higher than the CO_2/NH_3 baseline case, compared to the 9-fluids case achieving 15% improved COP for the same GWP. The middle point of the 9-fluids case (COP = 1.49, GWP = 30) is highlighted with a red circle in Figure 4 and detailed results are shown in Table 8. CO_2 and R1233zd(E) continued as the dominant fluids (47% and 51.8%) on the LTC whereas R600 remained dominant (87.9%) on the HTC. These fluids have the lowest GWPs (Table 3) of the chosen candidates and are very desirable for minimizing GWP. In the previous 9-fluids case, CO_2 emerged as the only dominant LTC fluid, whereas R1234ze(E) and R123 were the dominant ones on the HTC producing 11% higher COP, but at the cost of higher GWPs. When comparing the all-fluids cases with the non-phased-out cases, the maximum COPs achieved are lower for the non-phased-out cases, but the respective GWPs are also much lower. This is because the phased-out fluids have slightly higher performance but also significantly higher GWPs. Nevertheless, compared to the baseline cases, the optimal blends achieved higher simulated COPs and lower GWPs.

3.4.Conclusions

Refrigerant blend optimization was conducted using 30 fluids (15 LTC, 15 HTC) to develop blends which maximized system COP and minimized GWP for a two-stage cascade refrigeration system. All 30 fluids participated in the optimization in the first part and the same procedure was carried out for fluids which are not phased out by the US EPA (2015) in the second part. Significant improvement in COP and decrease in GWP was observed after optimizing blends on both sides of the cascade system and compared to the baseline cases. 49% increase in the system performance

(COP = 1.72, GWP = 395) was observed than the best baseline case when all 30 fluids were optimized whereas 32% increase (COP = 1.52, GWP = 70) was seen when only non-phased out fluids were considered. Minimum GWP of 2 was achieved during both cases but the range of GWP (2-70) was much lower when only non-phased out fluids were present. This type of analysis can be a good starting point to investigate the potential of new and low GWP refrigerant blends which can maximize system performance and minimize the environmental impact.

Chapter 4: Brazed Plate Heat Exchanger System Validation

Plate heat exchangers (PHXs) are widely employed in modern vapor compression systems due to their compact design, high thermal efficiency, and reduced refrigerant charge. They consist of multiple thin, corrugated metal plates arranged in a stack, where alternate channels carry hot and cold fluids. The plates provide a large surface area per unit volume, significantly enhancing heat transfer performance while minimizing the physical footprint of the equipment.

In vapor compression systems, PHXs are commonly used as evaporators, condensers, or economizers. Compared to traditional shell-and-tube or tube-fin HXs, PHXs offer superior heat transfer coefficients due to enhanced turbulence and reduced thermal resistance at the fluid-plate interface [59]. This makes them particularly advantageous in applications requiring high performance under compact and weight-constrained environments, such as heat pumps, chillers, and domestic water heating systems.

One of the key benefits of PHXs is their low refrigerant charge. Because of their narrow channel geometry and small internal volume, the amount of refrigerant required is significantly reduced—often by 30–50% compared to conventional designs [60]. Lower refrigerant charge leads to lower leakage and contributes to lower environmental impact, especially when using high-GWP refrigerants, and can also reduce system costs and enhance safety. This aligns with international regulatory trends aimed at minimizing greenhouse gas emissions from refrigerants (Kigali Amendment to the Montreal Protocol [17]).

The use of PHXs plays a crucial role in facilitating the adoption of low-GWP refrigerants such as R32 and R290, both of which are classified as mildly flammable (A2L) and highly flammable (A3), respectively. Due to their compactness and low internal volume, PHXs can significantly reduce the system refrigerant charge, thereby minimizing the flammability risk associated with larger refrigerant inventories [61]. Furthermore, integrating a secondary loop system — where the primary refrigerant circuit is confined to a sealed, compact zone and a secondary fluid such as water or glycol carries the cooling or heating load to the conditioned space — enhances safety by isolating the flammable refrigerants from occupied areas [62]. This approach not only allows compliance with evolving safety standards and regulations related to toxicity and flammability but also enables system designs that optimize performance with low-GWP refrigerants.

Accurate simulation and validation of vapor compression systems incorporating PHXs is crucial for several reasons. First, the complex two-phase flow and high heat transfer within PHXs require precise HX modeling to predict system capacity and COP. Second, PHXs are sensitive to fouling and pressure drop, both of which can degrade performance over time and must be accounted for in the design phase. Third, to fully leverage their benefits in system-level optimization, detailed validation using experimental data is required to ensure that simulation models represent real-world behavior, especially under off-design and transient conditions.

In this section, a brazed plate heat exchanger (BPHX) was modeled using an in-house PHX simulation platform developed by [45], [46]. Subsequently, a water source heat pump incorporating the BPHX as the condenser and using lower-GWP R32 as the refrigerant was validated against independent experimental data from a laboratory setting using a steady-state VC cycle simulation platform to demonstrate the accuracy and reliability of the platform in simulating VC systems with lower-GWP refrigerants and plate heat exchangers.

4.1.Cycle Description

The vapor compression cycle of interest is a water source heat pump with R32 acting as the primary fluid and water as the secondary fluid. This cycle utilizes BPHX as the condenser and a tube-fin heat exchanger (TFHX) as the evaporator. The basic cycle schematic is illustrated in Figure 5. The compressor in the system utilizes a ten-coefficient map as specified in AHRI 540 [63] and the expansion device's inlet subcooling and suction superheat are set as the convergence criteria.

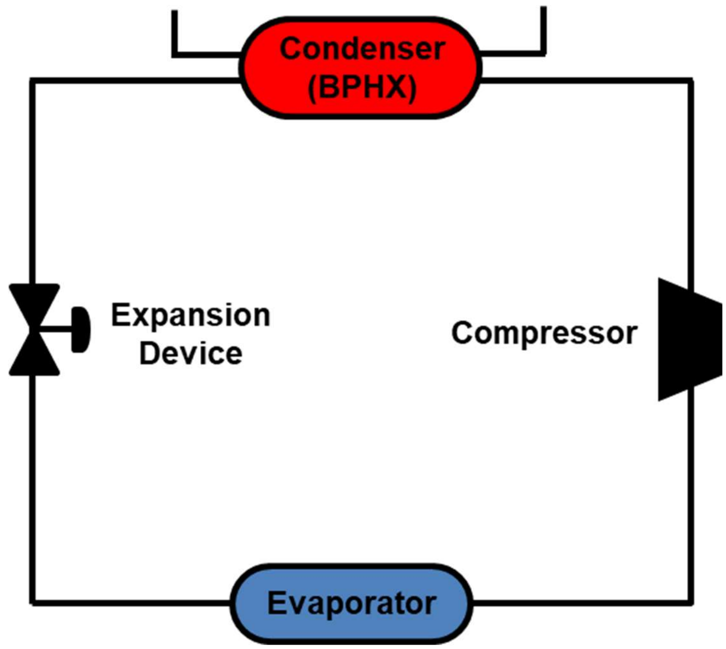

Figure 5. BPHX Cycle Schematic

4.2.Solver Description

In this work, we use a component model based steady state system simulation platform which was experimentally validated ([47], [48], [49]) to simulate the water source heat pump system. The simulation platform uses three main data structures to simulate a vapor compression system. These are components, ports, and junctions. Components are defined as refrigeration system components and are modeled as black box objects interacting with one another through a series of ports and junctions [48]. The cycle solving scheme used to solve the cycle is the enthalpy marching solver [49]. A nonlinear equation solver [64] is used in the current study to solve the residual equations derived from the mass and energy balance until convergence.

Additionally, the BPHX was modeled and simulated using an experimentally validated generalized PHX simulation platform ([45], [46]) that adopts a successive substitution approach where the

PHX is divided into a number of segments, M , of equal size and each segment can be solved individually. This platform has the flexibility to model a wide range of HX geometries and operating conditions rapidly and can be incorporated into the system solver to accurately predict system performance. Refrigerant thermodynamic property calculations utilize NIST REFPROP Version 9.1 [54] augmented with polynomial curve fits as proposed by [55].

4.3.Validation Results

The metrics of interest are system capacity, power (compressor) and mass flow rate and each quantity was normalized with respect to a maximum value (Figures 6, 7 and 8). The validation is conducted for a total of 19 points and the data was obtained from [65].

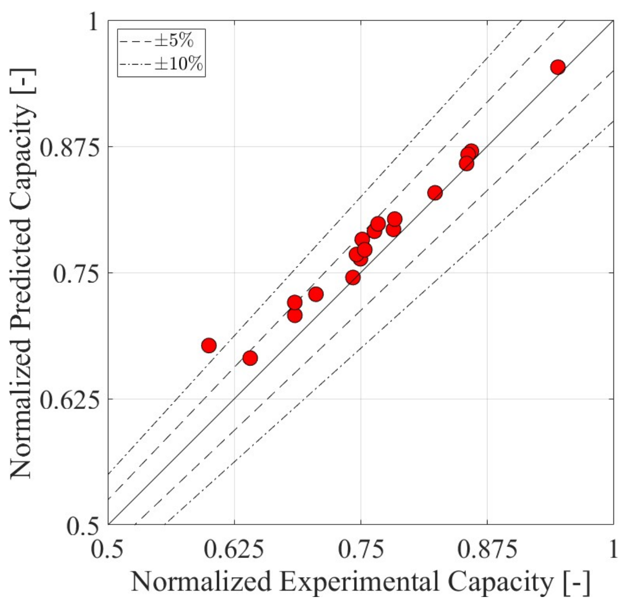

Figure 6. Simulated vs Experimental Capacity Normalized

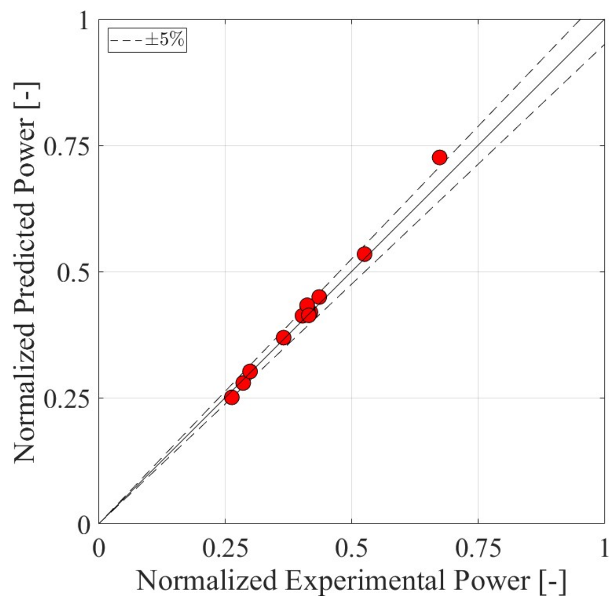

Figure 7. Simulated vs Experimental Power Normalized

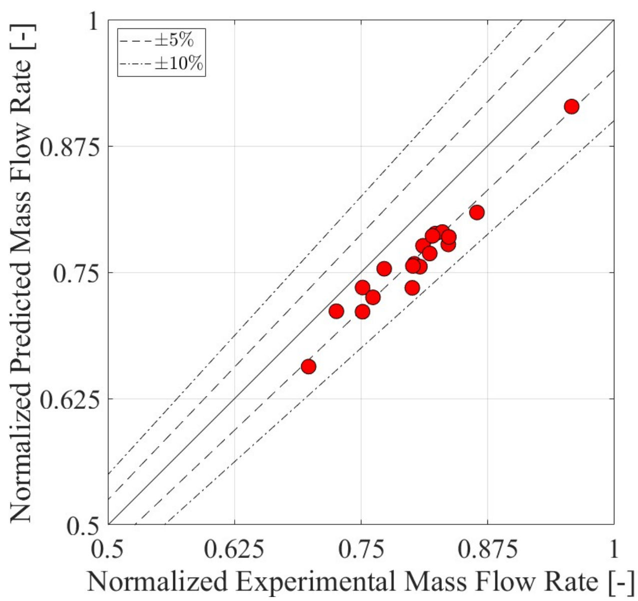

Figure 8. Simulated vs Experimental Mass Flow Rate Normalized

Table 9. Absolute Error Statistics

Statistic ↓ / Metric →	Capacity	Power	Mass Flow Rate
Min. APE (%)	0.39	0.16	1.96
Max. APE (%)	12.99	7.69	8.24
Median APE (%)	2.47	1.98	5.38

For all the three plots, the ±5% and ±10% deviation bands from the ideal parity line are shown to quantify the degree of agreement. The minimum, maximum and median absolute percentage errors (APE) are shown in Table 9 for capacity, power and mass flow rate. 18 out of 19 data points fell within ±5% of the measured values, demonstrating good prediction accuracy for capacity (Figure 6) with a min and max APE of 0.39 and 12.99% respectively (Table 9). However, a general trend of slight overprediction in capacity during the system simulation was observed.

Similarly, for power, 18 out of 19 data points fell within ±5% of the experimental values (Figure 7) with a min and max APE of 0.16 and 7.69% respectively (Table 9). 10 out of 19 data points were within the ±5% range for the mass flow rate prediction (Figure 8), with all remaining points falling to within 10%. The min and max APE for mass flow rate are 1.96 and 8.24% respectively (Table 9). A general trend of slight underprediction in the mass flow rate was observed during these runs. Also, correction factors for compressor power and mass flow rate based on the experimental data were applied to data points that initially exhibited higher deviations in these metrics, in alignment with standard industry practices for conducting similar model validations.

4.4.Conclusions

An experimental validation was conducted for a water source heat pump system using a BPHX as the condenser and R32 as the refrigerant. The results demonstrate overall good agreement between system simulation platform predictions and experimental measurements for capacity, power and mass flow rate with the average APE of 2.47, 1.98 and 5.38% (Table 9) respectively. These results demonstrate the accuracy and reliability of utilizing the steady-state simulation platform in predicting system performance and being a valuable tool for the design, analysis, and optimization of vapor compression systems, particularly those incorporating lower-GWP refrigerants and PHXs.

Chapter 5: Comprehensive System-Level Optimization Methodology for the Design of Air-to-Refrigerant HXs for Use of Lower GWP Refrigerants

Hydrocarbon (HC) refrigerants have emerged as promising replacements to hydrofluorocarbons due to their low GWP and promising thermophysical properties and R290 is one which was discussed in detail in the introduction section. Another refrigerant that is of interest is R32, which is being widely adopted as a low-GWP refrigerant in vapor compression systems, particularly in residential and light commercial applications ([66], [67] and [68]). With a GWP of 771, it offers a substantial reduction compared to R410A (GWP ≈ 2255), while providing similar thermal hydraulic performance [69]. Although R32's GWP is not as low as natural refrigerants like propane, it is classified as A2L - mildly flammable - making it less hazardous than highly flammable alternatives but still requiring charge control. In this section, a comprehensive system-level optimization methodology pertaining to fin geometry and tube geometry and circuitry was conducted to design tube-fin HXs with louver and slit fins. Next, an approximation-assisted optimization framework coupled with the optimization methodology was utilized to design HXs with shape-optimized, non-round tubes. The overall goal was to design optimal condenser and evaporator for using low GWP refrigerants R32 and R290 and to deliver similar performance as an R410A baseline air-conditioning system. To this end, system-level simulations were conducted to determine the best condenser/evaporator combination for minimizing overall system charge using an in-house experimentally validated steady state vapor compression system simulation platform. High level system metrics that include system COP, capacity, charge, etc. are discussed in detail for the systems employing these optimal HXs.

5.1.Cycle Description

The vapor compression cycle of interest is the 10.55 kW (3-Ton) air-to-refrigerant AC cycle which was experimentally validated by [50] for R410A and R32 refrigerants. The operating condition of interest is the AHRI A-Test condition [70]. This cycle utilizes tube-fin HXs as both the condenser and evaporator; the reader is referred to [70] for additional details. The basic cycle schematic is illustrated in Figure 9. All R410A and R32 system simulations utilized a ten-coefficient compressor map [63], while the R290 simulations utilized a generic efficiency-based compressor model [47]. The cycle configuration also includes pipes that account for heat loss and pressure drop representing the suction and liquid lines. The expansion device's inlet subcooling and suction superheat are the convergence criteria during the system simulation. The cycle subcooling and superheat are fixed at 2.79 K and 2.05 K for all R410A and R290 simulations whereas for R32, they are fixed at 1.35 K and 0.5 K respectively to match the experimental values by [50].

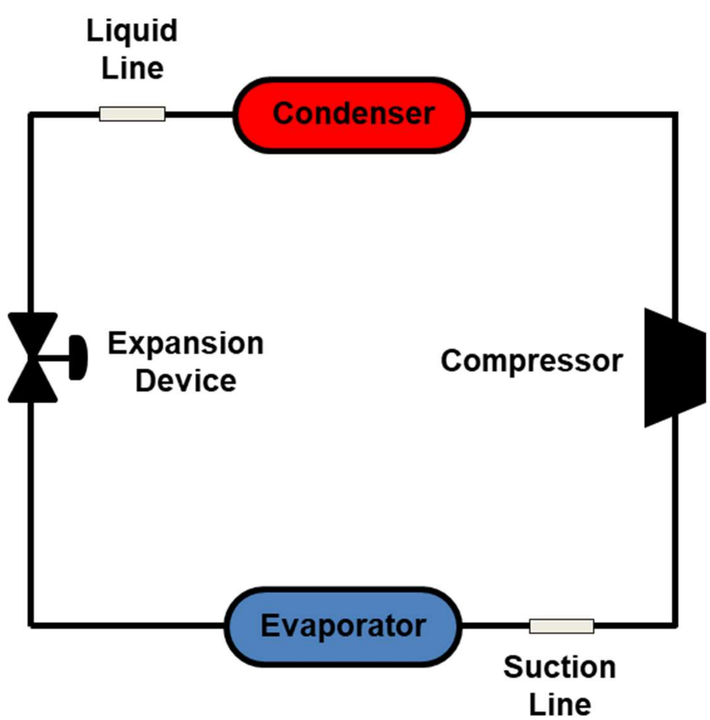

Figure 9. Baseline Cycle Schematic

5.2.Solver Description

The steady-state VC simulation platform used in this work was briefly discussed in section 4.2 of the thesis.

The HX simulations were done using an experimentally validated finite volume HX simulation platform [71]. This platform has the flexibility to model a wide range of air-to-refrigerant HX geometries and operating conditions rapidly and also can be incorporated into the system solver to accurately predict system performance. Refrigerant thermodynamic property calculations utilize NIST REFPROP Version 9.1 [54] augmented with polynomial curve fits as proposed by [55].

5.3.HX Component Optimization

5.3.1.Multi-Objective Optimization

MOGA [58] was used to conduct optimization. The MOGA settings are summarized in Table 10.

Table 10. MOGA settings

Metric	Value
Population Size	150
Population Replacement	30
Iterations	1000

5.3.2.Tube-Fin HXs Optimization Problem Description

This research considers air-to-refrigerant HXs in counterflow acting as condensers and evaporators with the refrigerants being R410A, R32 and R290. All HX models assume: (i) uniform normal air velocity and (ii) fully-developed uniform refrigerant flow. The louver fin type considered for the condenser and slit fin type is considered for the evaporator as it has better water drainage characteristics [72]. The heat transfer coefficients and pressure drop for each segment are computed using correlations given in Table 11 . For the air side correlations, correction factors recommended by [73] were used.

Table 11. TFHX Thermal-Hydraulic Performance Correlations

Working Fluid	HTC Correlation	ΔP Correlation
Air (Louver Fins)	Sarpotdar et al. (2016a) [74]	Sarpotdar et al. (2016a) [74]
Air (Slit Fins)	Sarpotdar et al. (2016b) [75]	Sarpotdar et al. (2016b) [75]
Liquid Refrigerant	Dittus & Boelter (1985) [76]	Blassius (1905) [77]
Two-phase Refrigerant	Condensation: Shah (2019) [78] Evaporation: Jung et al. (1989) [79]	Condensation: Xu-Fang (2013) [80] Evaporation: Xu-Fang (2012) [81]
Vapor Refrigerant	Dittus & Boelter (1985) [76]	Blassius (1905) [77]
Void Fraction Correlation: Yashar et al. (2001) [82]		

5.3.3.Tube-Fin HXs Optimization Problem Definition

This research considers a bi-objective optimization problem targeting minimum HX component envelope volume and airside pressure drop for both the condenser and evaporator (Eq. 3). The overall goal was to design both the condenser and the evaporator for using R32 and R290 and for the optimal HXs to deliver similar performance as the R410A baseline while reducing the HX envelope volume and the air side pressure drop being no larger than two times the baseline. The additional constraints for the HXs include the face area and refrigerant side pressure drop must not exceed the baseline values. There is one specific constraint pertaining to the condenser that the outlet subcooling must be at least equal to, but no more than 1.0 K higher than the baseline. The evaporator specific constraints include (i) the outlet superheat must be at least equal to, but no more than 1.0 K higher than the baseline and (ii) the sensible heat ratio must be within 10 percentage points of the baseline. In total, 8 continuous and 12 discrete design variables are considered pertaining to fin geometry and tube geometry and circuitry (Table 12).

Condenser	Evaporator	
$\min \Delta P_{air}; \min V_{HX}$ s.t. Fixed Inlet Fluid States / Flow Rates $\Delta T_{SC,BL} - 1.0\text{ K} \le \Delta T_{SC} \le \Delta T_{SC,BL}$ $\dot{Q} \ge \dot{Q}_{BL}; \quad A_f \le A_{BL} \cdot 1.85$ $\Delta P_{ref} \le 2 \cdot \Delta P_{ref,BL}; \quad \Delta P_{air} \le 2 \cdot \Delta P_{BL}$	$\min \Delta P_{air}; \min V_{HX}$ s.t. Fixed Inlet Fluid States / Flow Rates $\Delta T_{SH,BL} \le \Delta T_{SH} \le \Delta T_{SH,BL} + 1.0\text{ K}$ $\dot{Q} \ge \dot{Q}_{BL}; \quad A_f \le A_{BL} \cdot 1.25$ $\Delta P_{ref} \le 2 \cdot \Delta P_{ref,BL}; \quad \Delta P_{air} \le 2 \cdot \Delta P_{BL}$ $\lvert SHR - SHR_{BL} \rvert \le 0.1$	Eq. (3)

Table 12. Design Space for TFHXs

HX	Design Variable	Baseline	Range	Variable Type
Condenser	Tube OD (mm)	9.5	3-5	Discrete
	FPI (-)	21	14-40	Discrete
	Fin Type (-)	Wavy-Louver	Louver	-
	Louver pitch (mm)	-	0.8-1.8	Continuous
	Number of Louvers (-)	-	2-8	Discrete
	Tube Length (m)	2.16	1.5-3.0	Continuous
	Vertical Spacing Ratio (-)	2.632	1-2	Continuous
	Horizontal Spacing Ratio (-)	2.632	2-4	Continuous
	Number of Banks (-)	1	2-6	Discrete
	Number of Circuits (-)	6	4-131	Discrete
	Tubes per Circuit per Bank (-)	6	1-8	Discrete

Table Contd.

Evaporator	Tube OD (mm)	9.5	3-5	Discrete
	FPI (-)	15	14-40	Discrete
	Fin Type (-)	Wavy-Louver	Slit	-
	Slit Height / Fin Spacing	-	0.3-0.7	Continuous
	Number of Slits (-)	-	2-8	Discrete
	Tube Length (m)	0.503	0.15-1.0	Continuous
	Vertical Spacing Ratio (-)	2.105	1.1-2.0	Continuous
	Horizontal Spacing Ratio (-)	2.632	2-4	Continuous
	Number of Banks (-)	4	2-6	Discrete
	Number of Circuits (-)	4	4-131	Discrete
	Tubes per Circuit per Bank (-)	-	1-8	Discrete

5.3.4.Non-Round Tube HX Design & Optimization Framework

The experimentally-validated HX optimization framework of [42] was utilized to develop the optimal non-round tube HXs presented herein. The optimization framework (Figure 10) utilizes Approximation-Assisted Optimization (AAO) [83] involving automated CFD [84] and FEA simulations, Kriging metamodels [85], and optimization with MOGA [58]. The reader is referred to [42] for additional details on the development and validation of the optimization framework.

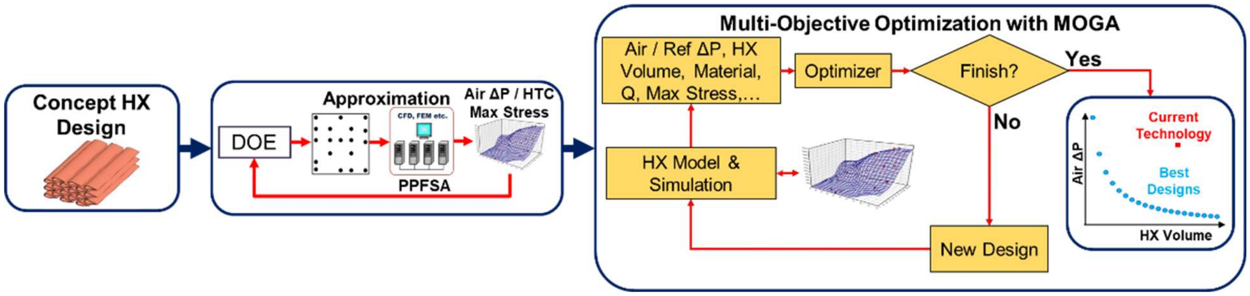

Figure 10. HX Optimization Framework [42]

5.3.5.Non-Round Tube HX Optimization Problem Description

For the non-round tube HXs, we consider only air-to-R290 HXs in crossflow acting as condensers and evaporators. All HX models assume: (i) uniform normal air velocity and (ii) fully-developed uniform refrigerant flow. The airside thermal-hydraulic performance is evaluated using CFD-based correlations and metamodels as outlined in [42], while the refrigerant-side thermal-hydraulic performance is calculated using existing small channel correlations for single-phase and two-phase flows (Table 13). The framework is utilized to design novel, finless air-to-R290 HXs for the AC system [50]. Generalized schematics for a finless HX with shape-optimized tubes and a generic tube-fin HX are shown in Figure **Error! Reference source not found.**11. The framework represents novel tube shapes (Figure 12) using fourth-order Non-Uniform Rational B-Splines (NURBS) [86].

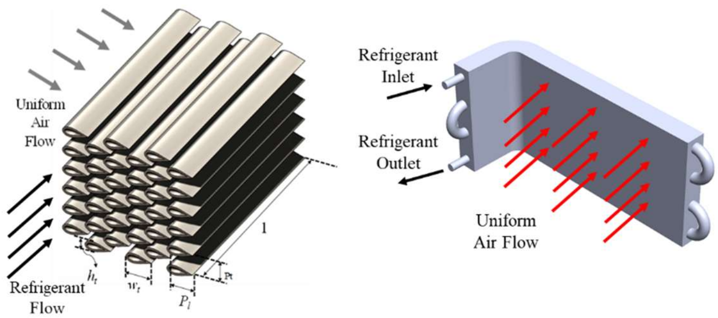

Figure 11. Schematic of (left) HX with Shape-Optimized Tubes; (right) Generic Tube-Fin Condenser

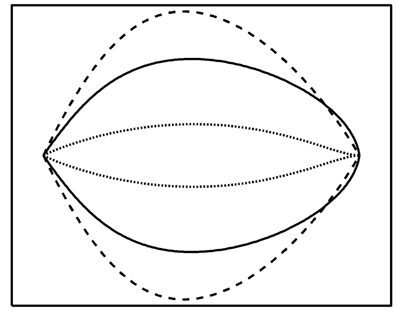

Figure 12. Sample NURBS shapes

Table 13. NTHX Thermal-Hydraulic Performance Correlations

Working Fluid	HTC Correlation	ΔP Correlation
Air	CFD Metamodels [42]	CFD Metamodels [42]
Liquid Refrigerant	Gnielinski (1976) [87]	Churchill (1977) [89]
Two-phase Refrigerant	Condensation: Shah (2019) [78] Evaporation: Shah (2017) [88]	Condensation: Xu-Fang (2013) [80] Evaporation: Xu-Fang (2012) [81]
Vapor Refrigerant	Gnielinski (1976) [87]	Churchill (1977) [89]
Void Fraction Correlation: Ali et at. (1993) [90]		

5.3.5.1.Tube Shape Considerations

The tube shape considered herein ([41], [42]) has been conventionally manufactured in both copper and aluminum [42]. The copper tubes show minimal deformation under internal pressures up to 20 MPa, thus validating the tube's structural strength [91]. We consider the copper version here.

5.3.6.Non-Round Tube HXs Optimization Problem Definition

Similar to the tube-fin HX optimization, a bi-objective optimization problem targeting minimum HX component envelope volume and airside pressure drop for both the condenser and evaporator (Eq. 4) is considered. The overall goal was to design air-to-R290 condensers/evaporators featuring conventionally manufactured, novel, non-round tubes [42] that meet capacity requirements while reducing envelope volume by at least 20%. All HXs have two fluid passes (condensers: 60%/40%, evaporators: 40%/60%). Additional constraints for both condenser and the evaporator include: (i) the HX height-to-length ratio is constrained to ensure a “nearly-square” HX face aspect ratio, i.e., no more than two times as large in one direction than the other; and (ii) the face area is constrained to be no larger than the baseline. There is one condenser-specific constraint: (i) the outlet subcooling must be at least the same, but no more than 1.0 K higher, than the baseline. There are two evaporator-specific constraints: (i) the outlet superheat must be at least the same, but no more than 1.0 K higher, than the baseline; and (ii) the sensible heat ratio must be within 3 percentage points of the baseline. In total, 14 continuous design variables are considered.

Condenser	**Evaporator**
$\min \Delta P_{air}; \min V_{HX}$	$\min \Delta P_{air}; \min V_{HX}$
s.t.	s.t.
Fixed Inlet Fluid States / Flow Rates	Fixed Inlet Fluid States / Flow Rates
Two fluid passes: 60% / 40%	Two fluid passes: 40% / 60%
$\Delta T_{SC,BL} - 1.0\text{ K} \le \Delta T_{SC} \le \Delta T_{SC,BL}$	$\Delta T_{SH,BL} \le \Delta T_{SH} \le \Delta T_{SH,BL} + 1.0\text{ K}$
$\dot{Q}_{BL} \le \dot{Q} \le 1.1 \cdot \dot{Q}_{BL}; \quad 0.5 \le H_{HX}/L_{HX} \le 2.0$	$\Delta P_{air} \le 20\text{ Pa}; \quad V_{HX} \le 0.8 \cdot V_{HX,BL}$
$\Delta P_{air} \le 20\text{ Pa}; \quad V_{HX} \le 0.8 \cdot V_{HX,BL}; \quad A_f \le A_{f,BL}$	$A_f \le A_{f,BL}; \quad 0.5 \le H_{HX}/L_{HX} \le 2.0$
	$\dot{Q}_{BL} \le \dot{Q} \le 1.1 \cdot \dot{Q}_{BL}; \quad \lvert SHR - SHR_{BL} \rvert \le 0.03$

Eq. (4)

5.4.System-Level Results

System-level simulations were conducted for all pairs of optimal condensers and evaporators to determine the best condenser/evaporator combination for minimizing overall system charge.

Metrics of interest include COP, capacity, power consumption (including the fan power consumption of both the HXs), sensible heat ratio, mass flow rate, total system charge, HX-level (condenser and evaporator) charge and internal volumes. In total, six cases are examined (Figure 13, 14 and 15), where all results are normalized with respect to the baseline systems with baseline tube-fin condenser and evaporator.

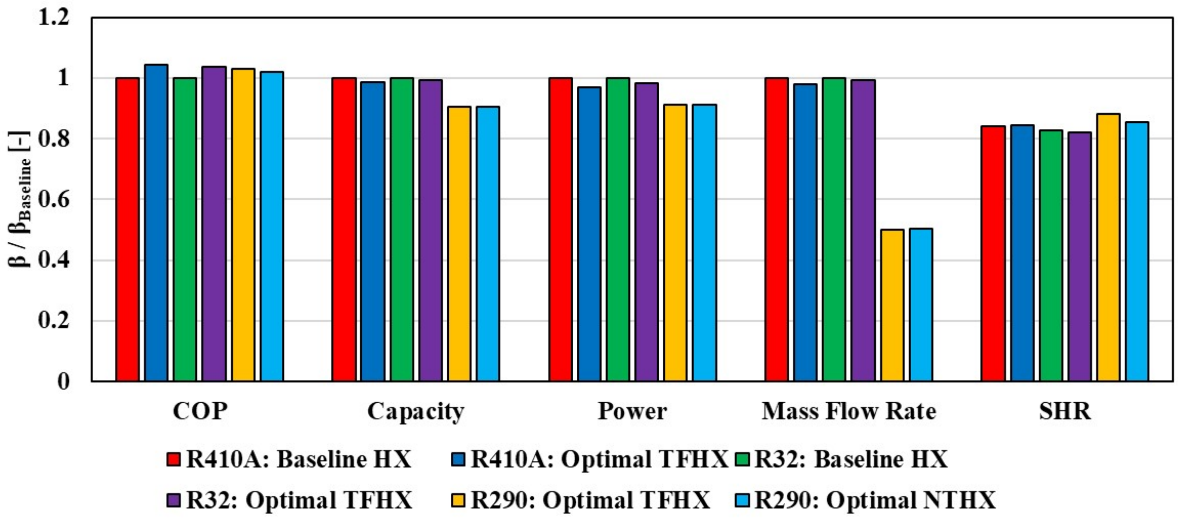

Figure 13. System-Level Metrics with Optimal HXs Compared to Baseline System HXs

Figure 13 illustrates the baseline systems utilizing R410A and R32, denoted by red and green bars, respectively. These systems employ baseline HXs and have been experimentally tested by [50] and for R290, there was no baseline AC system available. The first case of interest is replacing the baseline HXs with optimal TFHX keeping R410A as the refrigerant (dark blue bar in Figure 13). The predicted system capacity and power consumption reduced by 1% and 3% respectively, leading to a 4% increase in coefficient of performance (COP) compared to the baseline R410A system, while the refrigerant mass flow rate and sensible heat ratio (SHR) remain similar. The total refrigerant charge is 70% lower than the R410A baseline system (Figure 14) with 66% and 78% charge reduction in the condenser and the evaporator respectively. This reduction in charge is attributed to the fact that the total internal volume of the optimal R410A TFHXs is 57% lower than baseline HXs (Figure 15).

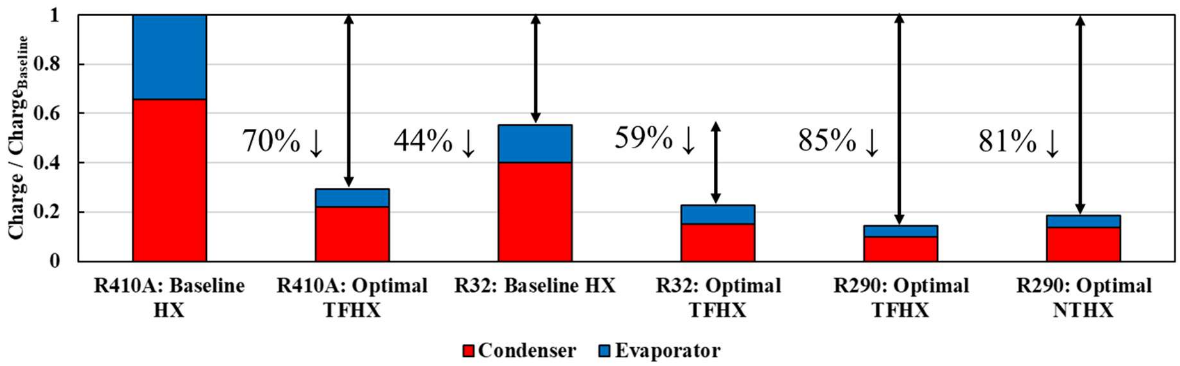

Figure 14. Charge Comparison Between Optimal HXs and Baseline HXs

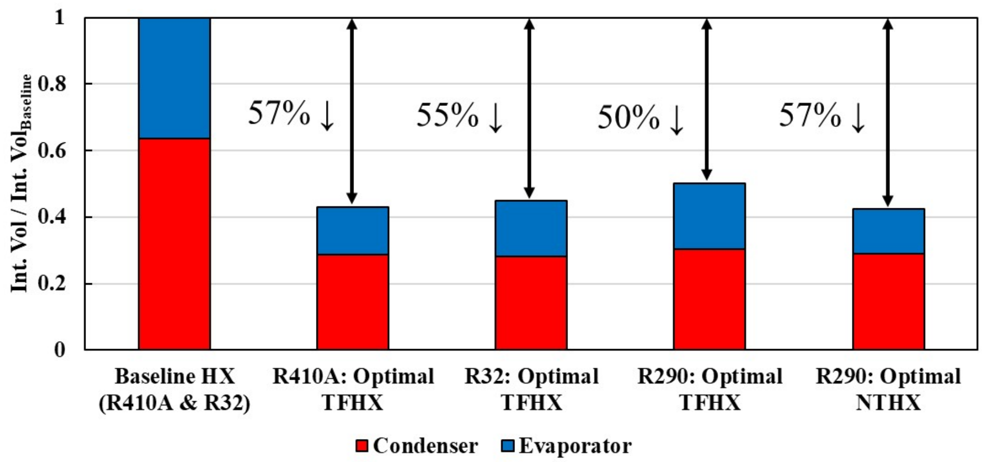

Figure 15. Internal Volume Comparison Between Optimal HXs and Baseline HXs

The second and third cases of relevance are those which utilize R32 with baseline HXs (green bar in Figure 13) and optimal TFHX (purple bar in Figure 13). The predicted system capacity, mass flow rate and SHR are similar to the baseline R32 case, but the total power consumption is 2% lower when using optimal TFHX resulting in a 3% increase in COP. Looking at total system charge, there is a 44% decrease when we replace the refrigerant from R410A to R32 using baseline HXs (Figure 14) and this is due to R32 having 30% [92] lower density than R410A. Furthermore, utilizing the optimal TFHX with 55% reduction in total internal volume (Figure 15), there is a 59%

decrease in the total system charge (in-addition to using R32 using baseline HXs) with a 62% decrease in the condenser and a 50% decrease in the evaporator.

The final two cases of interest are those which utilize R290 with optimal TFHX and optimal non-round tube heat exchangers (NTHX). Upon employing the optimal TFHX and looking at the high-level system metrics, the predicted system capacity was about 10% lower than the R410A baseline; the predicted overall system COP was slightly higher than the baseline R410A system due to the predicted system power consumption reducing by about 9% and SHR was four percentage points higher (orange bar in Figure 13). Most notably, the reduction in the total system charge is staggering with 85% – the best optimal tube-fin condenser achieved about an 84% lower component-level refrigerant charge reduction, while the best optimal evaporator achieved about an 87% component-level refrigerant charge reduction (Figure 14). This is in line with the 50% reduction in the total internal volume of the optimal TFHXs (Figure 15). When we replace the optimal TFHXs with optimal NTHXs, both the predicted system capacity and total power consumption reduced by 9%, culminating in an 2% increase in COP with SHR being similar (light blue bar in Figure 13) when compared to the baseline R410A system. With the total internal volume of the NTHXs being 57% lower (Figure 15) compared to the baseline HXs, the predicted total system refrigerant charge reduction is approximately 81%, with a 79% and 85% decrease in the condenser and the evaporator respectively (Figure 14). However, it should be noted that this work considers only the refrigerant charge in the HX (tube) core, not the headers. Previous work has shown that headers can contain an additional 10-20% refrigerant charge on top of that in the HX core [93]. Nevertheless, the estimated charge reduction (excluding headers) is up to 80%, and an additional 20% refrigerant charge from the headers would still yield more than 70% refrigerant charge reductions compared to the baseline HXs. Also, the charge reductions in the condenser were the highest compared to the evaporator since the condenser contains more refrigerant charge than the evaporator (resulting from subcooled liquid refrigerant). Additionally, the predicted mass flow rate for both the cases is about 50% lower (Figure 13), which is directly related to R290 having a higher latent heat of vaporization compared to R410A at the same evaporating temperature.

5.5.Conclusions

In this section, a comprehensive system-level optimization methodology was developed for the rapid design of air-to-refrigerant tube-fin and non-round tube HXs to facilitate the transition to lower GWP refrigerants R32 and R290. To demonstrate the performance of these optimal HXs, system simulations were conducted for an air-to-refrigerant AC system. System simulations considering the optimal TFHXs that have lower total internal volume with R32 and R290 predicted similar performance in terms of capacity and COP to the baseline R410A system along with significant system refrigerant charge reductions up to 77% and 85% for R32 and R290 respectively. Next, the novel, shape-optimized, non-round tube geometry used herein is conventionally manufacturable and results in smaller HXs with similar performance which utilize less material and refrigerant charge compared to the baseline HXs. The system performance of the optimal NTHXs with R290 in terms of capacity and COP are similar to the baseline R410A system with refrigerant charge reductions by up to a staggering 81% was observed. The above analysis further emphasizes the benefits of R32 and R290 over R410A: when the HXs in a system are properly-designed HXs, R32 and R290 can enable significant refrigerant charge reductions compared to R410A, which is a critical safety and environmental objective in the context of enabling the use of lower GWP but flammable refrigerants in HVAC&R systems. Furthermore, it is clear that mathematically-rigorous optimization is one pathway towards redesigning HXs for this purpose. The promising system-level performance and charge reductions presented herein will help facilitate the transition to lower GWP, natural refrigerants such as R290.

Chapter 6: Conclusions and Future Work

6.1. Summary and Conclusions

This section comprises a brief summary of each research objective pertaining to this thesis

(i) Multi-Objective Optimization of Refrigerant Blends for Supermarket Systems: In Chapter 3, a two-stage cascade system was thermodynamically modeled, and a multi-objective optimization study was conducted to design optimal refrigerant blends to maximize COP and minimize GWP of the system. Significant improvements in COP by up to 49% (COP = 1.72, GWP = 395 – compared to CO_2/NH_3 baseline COP of 1.15) and decreases in GWP (COP = 1.33, GWP = 2) were achieved when the optimal blends were utilized in the system.

(ii) Water Source Heat Pump System Validation: In Chapter 4, an experimental validation was conducted for a lower-GWP R32 water source heat pump system based on brazed plate and air-to-refrigerant HXs utilizing a steady-state VC system simulation platform. The validation results showed good agreement, with 18 out of 19 points for both capacity and power falling within ±5% of the measured values.

(iii) Comprehensive System-Level Optimization Methodology for the Design of Air-to-Refrigerant HXs for Use of Lower GWP Refrigerants: In Chapter 5, a comprehensive investigation of HX design space (for e.g. tube diameters, spacings, pitches, etc.) was conducted and an optimization methodology was developed to design tube-fin and non-round tube HXs to facilitate the transition to lower-GWP refrigerants R32 and R290.

System simulations showed significant refrigerant charge reductions up to 77% and 85% for R32 and R290 using optimal TFHXs and 81% when using the NTHXs with similar COP and capacity to the baseline.

6.2.Contributions

The main contributions of this thesis are

(i) An optimization methodology was developed to design novel refrigerant blends that improve efficiency while lowering the GWP of the blends for the system, enabling rapid and effective blend optimization for vapor compression systems

(ii) Experimental validation was conducted for an R32 water source heat pump with a mix of brazed plate and air-to-refrigerant HXs demonstrating the steady-state VC system platform's good accuracy and robustness in predicting system performance incorporating lower-GWP refrigerants and PHXs.

(iii) A comprehensive system-level optimization methodology was developed for air-to-refrigerant HXs that can enable design of high performance optimal HXs pairs (i.e., condenser and evaporator) and carry low refrigerant charge. This will also facilitate industry transition to lower GWP refrigerants and reduce life cycle climate impact.

6.3.Future Work

This thesis aims to deliver effective solutions pertaining to refrigerant blend optimization in VC systems and utilize high performance HXs that utilize less refrigerant charge to enable usage of low GWP refrigerants. The following features and directions would further advance the work conducted in this thesis:

- Including flammability calculations for the refrigerant blends that can be set as an objective or a constraint will truly unlock the potential of developing refrigerant blends for a selected system.
- From a simulation perspective, conducting simultaneous system-level optimization of both the condenser and evaporator would result in optimal HX pairs which could improve (as opposed to maintaining) the COP. Additionally, as the HXs become smaller, the system including connecting piping can also be made smaller, further reducing refrigerant charge.
- Validation of optimal system designs from system-level HX optimization study

6.3.List of Publications

- [94] **Meruva, V.P**., Tancabel, J., Aute, V., 2024. "Design Optimization of Heat Exchangers utilizing Shape-Optimized, Non-Round Tubes for a Residential Air-Conditioning System using R290". 16th IIR-Gustav Lorentzen Conference on Natural Refrigerants, International Institute of Refrigeration, College Park, MD, USA. DOI: http://dx.doi.org/10.18462/iir.gl.2024.1241
- [95] **Meruva, V.P**., Tancabel, J., Aute, V., 2024. "Multi-Objective Optimization of Refrigerant Blends for Supermarket Systems". 8th IIR International Conference on Sustainability and the Cold Chain, International Institute of Refrigeration, Tokyo, Japan. DOI: https://dx.doi.org/10.18462/iir.iccc2024.1044

Bibliography

[1] "U.S. energy consumption by source and sector, 2023".

[2] "Frequently Asked Questions (FAQs) - U.S. Energy Information Administration (EIA)." Accessed: Apr. 28, 2025. [Online]. Available: https://www.eia.gov/tools/faqs/faq.php?id=1174&t=1

[3] "U.S. Energy Information Administration - EIA - Independent Statistics and Analysis." Accessed: Apr. 28, 2025. [Online]. Available: https://www.eia.gov/pressroom/releases/press535.php

[4] H. M. Getu and P. K. Bansal, "Thermodynamic analysis of an R744–R717 cascade refrigeration system," *International Journal of Refrigeration*, vol. 31, no. 1, pp. 45–54, Jan. 2008, doi: 10.1016/j.ijrefrig.2007.06.014.

[5] M. Pan, H. Zhao, D. Liang, Y. Zhu, Y. Liang, and G. Bao, "A Review of the Cascade Refrigeration System," *Energies*, vol. 13, no. 9, Art. no. 9, Jan. 2020, doi: 10.3390/en13092254.

[6] J. Alberto Dopazo, J. Fernández-Seara, J. Sieres, and F. J. Uhía, "Theoretical analysis of a CO2–NH3 cascade refrigeration system for cooling applications at low temperatures," *Applied Thermal Engineering*, vol. 29, no. 8–9, pp. 1577–1583, Jun. 2009, doi: 10.1016/j.applthermaleng.2008.07.006.

[7] T.-S. Lee, C.-H. Liu, and T.-W. Chen, "Thermodynamic analysis of optimal condensing temperature of cascade-condenser in CO2/NH3 cascade refrigeration systems," *International Journal of Refrigeration*, vol. 29, no. 7, pp. 1100–1108, Nov. 2006, doi: 10.1016/j.ijrefrig.2006.03.003.

[8] J. A. Dopazo and J. Fernández-Seara, “Experimental evaluation of a cascade refrigeration system prototype with CO2 and NH3 for freezing process applications,” *International Journal of Refrigeration*, vol. 34, no. 1, pp. 257–267, Jan. 2011, doi: 10.1016/j.ijrefrig.2010.07.010.

[9] Y. Xie, C. Liu, L. Lun, and X. Zhang, “Use of R290/R170 in Lieu of R22/R23 in Cascade Refrigeration Cycle,” Jul. 2008.

[10] Z. Sun, Q. Wang, Z. Xie, S. Liu, D. Su, and Q. Cui, “Energy and exergy analysis of low GWP refrigerants in cascade refrigeration system,” *Energy*, vol. 170, pp. 1170–1180, Mar. 2019, doi: 10.1016/j.energy.2018.12.055.

[11] C. Aktemur, I. T. Ozturk, and C. Cimsit, “Comparative energy and exergy analysis of a subcritical cascade refrigeration system using low global warming potential refrigerants,” *Applied Thermal Engineering*, vol. 184, p. 116254, Feb. 2021, doi: 10.1016/j.applthermaleng.2020.116254.

[12] J. M. Calm, “The next generation of refrigerants – Historical review, considerations, and outlook,” *International Journal of Refrigeration*, vol. 31, no. 7, pp. 1123–1133, Nov. 2008, doi: 10.1016/j.ijrefrig.2008.01.013.

[13] P. A. Domanski, R. Brignoli, J. S. Brown, A. F. Kazakov, and M. O. McLinden, “Low-GWP refrigerants for medium and high-pressure applications,” *International Journal of Refrigeration*, vol. 84, pp. 198–209, Dec. 2017, doi: 10.1016/j.ijrefrig.2017.08.019.

[14] A. Mota-Babiloni, J. Haro-Ortuño, J. Navarro-Esbrí, and Á. Barragán-Cervera, “Experimental drop-in replacement of R404A for warm countries using the low GWP mixtures R454C and R455A,” *International Journal of Refrigeration*, vol. 91, pp. 136–145, Jul. 2018, doi: 10.1016/j.ijrefrig.2018.05.018.

[15] L. H. P. Massuchetto, R. B. C. do Nascimento, S. M. R. de Carvalho, H. V. de Araújo, and J. V. H. d'Angelo, "Thermodynamic performance evaluation of a cascade refrigeration system with mixed refrigerants: R744/R1270, R744/R717 and R744/RE170," *International Journal of Refrigeration*, vol. 106, pp. 201–212, Oct. 2019, doi: 10.1016/j.ijrefrig.2019.07.005.

[16] B. Yu, H. Ouyang, J. Shi, W. Liu, and J. Chen, "Evaluation of low-GWP and mildly flammable mixtures as new alternatives for R410A in air-conditioning and heat pump system," *International Journal of Refrigeration*, vol. 121, pp. 95–104, Jan. 2021, doi: 10.1016/j.ijrefrig.2020.09.018.

[17] "ratification_kigali.pdf." Accessed: Apr. 28, 2025. [Online]. Available: https://ozone.unep.org/sites/default/files/2019-08/ratification_kigali.pdf

[18] "EU-Rules - Fluorinated Greenhouse Gases – Climate Action." Accessed: Apr. 28, 2025. [Online]. Available: https://climate.ec.europa.eu/eu-action/fluorinated-greenhouse-gases/f-gas-legislation_en

[19] S. Yadav, J. Liu, and S. C. Kim, "A comprehensive study on 21st-century refrigerants - R290 and R1234yf: A review," *International Journal of Heat and Mass Transfer*, vol. 182, p. 121947, Jan. 2022, doi: 10.1016/j.ijheatmasstransfer.2021.121947.

[20] "ISO 5149-1:2014," ISO. Accessed: Apr. 28, 2025. [Online]. Available: https://www.iso.org/standard/54979.html

[21] "IEC 60335-1:2020." Accessed: Apr. 28, 2025. [Online]. Available: https://webstore.iec.ch/en/publication/61880

[22] "EN IEC 60335-2-89:2022 - Household and similar electrical appliances - Safety - Part 2-89: Particular requirements for commercial refrigerating appliances and ice-makers with an incorporated or remote refrigerant unit or motor-compressor," iTeh Standards. Accessed: Apr. 28,

2025. [Online]. Available: https://standards.iteh.ai/catalog/standards/clc/1a169cb9-c73f-4c7c-bdc3-e6b62e387f54/en-iec-60335-2-89-2022

[23] "UL 60335-2-89 | UL Standards & Engagement | UL Standard." Accessed: Apr. 28, 2025. [Online]. Available: https://www.shopulstandards.com/ProductDetail.aspx?UniqueKey=40821

[24] "IEC 60335-2-89:2019." Accessed: Apr. 28, 2025. [Online]. Available: https://webstore.iec.ch/en/publication/62243

[25] "IEC 60335-2-24:2020." Accessed: Apr. 28, 2025. [Online]. Available: https://webstore.iec.ch/en/publication/65317

[26] "ISO 5149-4:2022," ISO. Accessed: Apr. 28, 2025. [Online]. Available: https://www.iso.org/standard/82475.html

[27] L. J. M. Kuijpers, J. A. de Wit, and M. J. P. Janssen, "Possibilities for the replacement of CFC 12 in domestic equipment," *International Journal of Refrigeration*, vol. 11, no. 4, pp. 284–291, Jul. 1988, doi: 10.1016/0140-7007(88)90088-6.

[28] G. A. Longo, S. Mancin, G. Righetti, and C. Zilio, "Hydrocarbon refrigerants HC290 (Propane) and HC1270 (Propylene) low GWP long-term substitutes for HFC404A: A comparative analysis in vaporisation inside a small-diameter horizontal smooth tube," *Applied Thermal Engineering*, vol. 124, pp. 707–715, Sep. 2017, doi: 10.1016/j.applthermaleng.2017.06.080.

[29] K. Mani and V. Selladurai, "Experimental analysis of a new refrigerant mixture as drop-in replacement for CFC12 and HFC134a," *International Journal of Thermal Sciences*, vol. 47, no. 11, pp. 1490–1495, Nov. 2008, doi: 10.1016/j.ijthermalsci.2007.11.008.

[30] K. Nawaz, J. Rendall, A. Elatar, and J. Sun, "Propane As Working Fluid For Heat Pump Water Heaters- Opportunities And Challenges," 2022.

[31] W. S. Mohammad and A. Oda Jassim, “Experimental and Theoretical Investigation of Propane/Butane and Propane/Isobutane Mixtures as an Alternative to R134a in a Domestic Refrigerator,” *Engineering and Technology Journal*, vol. 32, no. 5, pp. 1266–1286, Jun. 2014, doi: 10.30684/etj.32.5A.15.

[32] Themefisher, “LC150,” LC150. Accessed: Apr. 28, 2025. [Online]. Available: https://lc150.eu/

[33] S. Chen, J. F. Judge, E. A. Groll, and R. Radermacher, “Theoretical Analysis of Hydrocarbon Refrigerant Mixtures as a Replacement for HCFC -22 for Residential Uses,” 1994.

[34] J. P. Meyer, “THE PERFORMANCE OF THE REFRIGERANTS R-134a, R-290, R404A, R-407c AND R-4I0A IN AIR CONDITIONERS AND REFRIGERATORS,” 2000.

[35] P. Fernando, B. Palm, P. Lundqvist, and E. Granryd, “Propane heat pump with low refrigerant charge: design and laboratory tests,” *International Journal of Refrigeration*, vol. 27, no. 7, pp. 761–773, Nov. 2004, doi: 10.1016/j.ijrefrig.2004.06.012.

[36] A. S. Padalkar, K. V. Mali, and S. Devotta, “Simulated and experimental performance of split packaged air conditioner using refrigerant HC-290 as a substitute for HCFC-22,” *Applied Thermal Engineering*, vol. 62, no. 1, pp. 277–284, Jan. 2014, doi: 10.1016/j.applthermaleng.2013.09.017.

[37] T. K. Berkah Fajar, P. Restu Bagas, S. Ukhi, M. I. Alhamid, and A. Lubis, “Energy and exergy analysis of an R410A small vapor compression system retrofitted with R290,” *Case Studies in Thermal Engineering*, vol. 21, p. 100671, Oct. 2020, doi: 10.1016/j.csite.2020.100671.

[38] J. Tancabel, V. C. Aute, and R. Radermacher, “Review of Shape and Topology Optimization for Design of Air-to-Refrigerant Heat Exchangers,” 2018.

[39] “Rational approach to refrigerant charge reduction. - pap. n. 1832.” Accessed: Apr. 28, 2025. [Online]. Available: https://iifiir.org/en/fridoc/rational-approach-to-refrigerant-charge-reduction-35146

[40] W. M. Kays and A. L. London, “Compact heat exchangers,” Jan. 1984, Accessed: Apr. 28, 2025. [Online]. Available: https://www.osti.gov/biblio/6132549

[41] D. Bacellar, Aute ,Vikrant, Huang ,Zhiwei, and R. and Radermacher, “Design optimization and validation of high-performance heat exchangers using approximation assisted optimization and additive manufacturing,” *Science and Technology for the Built Environment*, vol. 23, no. 6, pp. 896–911, Aug. 2017, doi: 10.1080/23744731.2017.1333877.

[42] J. Tancabel *et al.*, “Multi-scale and multi-physics analysis, design optimization, and experimental validation of heat exchangers utilizing high performance, non-round tubes,” *Applied Thermal Engineering*, vol. 216, p. 118965, Nov. 2022, doi: 10.1016/j.applthermaleng.2022.118965.

[43] T. J, A. V, and L. J, “Optimization of R290 heat exchangers utilizing high performance, non-round tubes.,” 14th IIR-Gustav Lorentzen Conference on Natural Refrigerants (GL2020). Proceedings. Kyoto, Japon, December 7-9th 2020. Accessed: Apr. 28, 2025. [Online]. Available: https://iifiir.org/en/fridoc/optimization-of-r290-heat-exchangers-utilizing-high-performance-142980

[44] O. US EPA, “Ozone-Depleting Substances.” Accessed: Dec. 11, 2023. [Online]. Available: https://www.epa.gov/ozone-layer-protection/ozone-depleting-substances

[45] H. Qiao, V. Aute, H. Lee, K. Saleh, and R. Radermacher, “A new model for plate heat exchangers with generalized flow configurations and phase change,” *International Journal of Refrigeration*, vol. 36, no. 2, pp. 622–632, Mar. 2013, doi: 10.1016/j.ijrefrig.2012.11.020.

[46] R. Eldeeb, V. Aute, and R. Radermacher, “An Improved Approach for Modeling Plate Heat Exchangers Based on Successive Substitution in Alternating Flow Directions,” 2016.

[47] D. H. Richardson, H. Jiang, D. Lindsay, and R. Radermacher, “Optimization Of Vapor Compression Systems Via Simulation”.

[48] J. Winkler, V. Aute, and R. Radermacher, “Component-Based Vapor Compression Simulation Tool With Integrated Multi-Objective Optimization Routines,” 2006.

[49] J. Winkler, V. Aute, and R. Radermacher, “Comprehensive investigation of numerical methods in simulating a steady-state vapor compression system,” *International Journal of Refrigeration*, vol. 31, no. 5, pp. 930–942, Aug. 2008, doi: 10.1016/j.ijrefrig.2007.08.008.

[50] A. Alabdulkarem, R. Eldeeb, Y. Hwang, V. Aute, and R. Radermacher, “Testing, simulation and soft-optimization of R410A low-GWP alternatives in heat pump system,” *International Journal of Refrigeration*, vol. 60, pp. 106–117, Dec. 2015, doi: 10.1016/j.ijrefrig.2015.08.001.

[51] Z. Meng, H. Zhang, J. Qiu, and M. Lei, “Theoretical analysis of R1234ze(E), R152a, and R1234ze(E)/R152a mixtures as replacements of R134a in vapor compression system,” *Advances in Mechanical Engineering*, vol. 8, no. 11, p. 1687814016676945, Nov. 2016, doi: 10.1177/1687814016676945.

[52] “IPCC_AR6_WGI_Chapter_07_Supplementary_Material.pdf.” Accessed: Apr. 03, 2024. [Online]. Available: https://www.ipcc.ch/report/ar6/wg1/downloads/report/IPCC_AR6_WGI_Chapter_07_Supplementary_Material.pdf

[53] "Global warming potential (GWP) of HFC refrigerants." Accessed: Dec. 11, 2023. [Online]. Available: https://iifiir.org/en/encyclopedia-of-refrigeration/global-warming-potential-gwp-of-hfc-refrigerants

[54] E. W. Lemmon, M. L. Huber, and M. O. McLinden, "NIST Standard Reference Database 23: Reference Fluid Thermodynamic and Transport Properties-REFPROP, Version 9.1," *NIST*, May 2013, Accessed: Dec. 17, 2023. [Online]. Available: https://www.nist.gov/publications/nist-standard-reference-database-23-reference-fluid-thermodynamic-and-transport

[55] V. Aute and R. Radermacher, "Standardized Polynomials for Fast Evaluation of Refrigerant Thermophysical Properties," 2014.

[56] A. Kilicarslan and M. Hosoz, "Energy and irreversibility analysis of a cascade refrigeration system for various refrigerant couples," *Energy Conversion and Management*, vol. 51, no. 12, pp. 2947–2954, Dec. 2010, doi: 10.1016/j.enconman.2010.06.037.

[57] V. K. Gupta, "Numerical optimization of multi-stage cascaded refrigeration-heat pump system," *Journal of Heat Recovery Systems*, vol. 5, no. 4, pp. 305–319, Jan. 1985, doi: 10.1016/0198-7593(85)90005-0.

[58] K. Deb, *Multi-objective optimization using evolutionary algorithms*, Reprint. in Wiley paperback series. Chichester Weinheim: Wiley, 2009.

[59] S. Kakaç, H. Liu, and A. Pramuanjaroenkij, *Heat Exchangers: Selection, Rating, and Thermal Design, Second Edition*, 2nd ed. Boca Raton: CRC Press, 2002. doi: 10.1201/9781420053746.

[60] Z. H. Ayub, "Plate Heat Exchanger Literature Survey and New Heat Transfer and Pressure Drop Correlations for Refrigerant Evaporators," *Heat Transfer Engineering*, vol. 24, no. 5, pp. 3–16, Sep. 2003, doi: 10.1080/01457630304056.

[61] L. Schnabel, T. Methler, A. H. Hassan, C. Dankwerth, and J. M. G. Maciá, "Design and Analysis of Charge-Reduced Refrigerant Cycles Using R290," *Chemie Ingenieur Technik*, vol. 95, no. 3, pp. 353–362, 2023, doi: 10.1002/cite.202200150.

[62] "Secondary Loop Residential Heat Pump Design, Performance, and Cost Analysis Utilizing R290 - ProQuest." Accessed: Apr. 28, 2025. [Online]. Available: https://www.proquest.com/docview/2017207720?pq-origsite=gscholar&fromopenview=true&sourcetype=Dissertations%20&%20Theses

[63] "AHRI_Standard_540_(I-P_and_SI)_2020_Standard_for_Performance_Rating_of_Positive_Displacement_Refrigerant_Compressors_and_Compressor_Units.pdf." Accessed: Apr. 28, 2025. [Online]. Available: https://www.ahrinet.org/system/files/2023-06/AHRI_Standard_540_%28I-P_and_SI%29_2020_Standard_for_Performance_Rating_of_Positive_Displacement_Refrigerant_Compressors_and_Compressor_Units.pdf

[64] "Scopus - Document details - A class of methods for solving nonlinear simultaneous equations." Accessed: Apr. 28, 2025. [Online]. Available: https://www.scopus.com/record/display.uri?eid=2-s2.0-84968510937&origin=inward

[65] "Private Communications, 2025."

[66] A. Mota-Babiloni, J. Navarro-Esbrí, P. Makhnatch, and F. Molés, "Refrigerant R32 as lower GWP working fluid in residential air conditioning systems in Europe and the USA," *Renewable and Sustainable Energy Reviews*, vol. 80, pp. 1031–1042, Dec. 2017, doi: 10.1016/j.rser.2017.05.216.

[67] B. O. Bolaji, "Experimental study of R152a and R32 to replace R134a in a domestic refrigerator," *Energy*, vol. 35, no. 9, pp. 3793–3798, Sep. 2010, doi: 10.1016/j.energy.2010.05.031.

[68] T. Sutandi, A. S. Margana, K. Sumeru, and M. F. Sukri, "Experimental Study of R32 as a Retrofit for R410A Refrigerant in a Residential Air Conditioner," presented at the International Seminar of Science and Applied Technology (ISSAT 2020), Atlantis Press, Dec. 2020, pp. 167–170. doi: 10.2991/aer.k.201221.029.

[69] M. Lee, S. Lee, J. Yeob Chung, S. Kwon, and Y. Kim, "Energy and environmental performances of heat pumps using R32 and R466A as alternatives to R410A," *Applied Thermal Engineering*, vol. 256, p. 124140, Nov. 2024, doi: 10.1016/j.applthermaleng.2024.124140.

[70] "AHRI Standard 210.240-2023 (2020).pdf." Accessed: Apr. 28, 2025. [Online]. Available: https://www.ahrinet.org/system/files/2024-04/AHRI%20Standard%20210.240-2023%20%282020%29.pdf

[71] H. Jiang, V. Aute, and R. Radermacher, "CoilDesigner: a general-purpose simulation and design tool for air-to-refrigerant heat exchangers," *International Journal of Refrigeration*, vol. 29, no. 4, pp. 601–610, Jun. 2006, doi: 10.1016/j.ijrefrig.2005.09.019.

[72] W. Sheng, X. Li, R. Wang, C. Dang, and M. Song, "Condensate drainage on slit or louvered fins in microchannel heat exchangers for anti-frosting," *Energy and Buildings*, vol. 223, p. 110215, Sep. 2020, doi: 10.1016/j.enbuild.2020.110215.

[73] D. Nasuta, "Experimental Validation of CFD-Based Correlations for 5 mm Louver- and Slit-Fin Heat Exchangers: Lessons Learned," 2018.

[74] S. Sarpotdar, "CFD-Based Airside Heat Transfer and Pressure Drop Correlation Development for Small Diameter (3 mm to 5 mm) Louver Fin Heat Exchangers," 2016.

[75] S. Sarpotdar, “CFD Based Comparison of Slit Fin and Louver Fin Performance for Small Diameter (3mm to 5 mm) Heat Exchangers,” 2016.

[76] F. W. Dittus and L. M. K. Boelter, “Heat transfer in automobile radiators of the tubular type,” *International Communications in Heat and Mass Transfer*, vol. 12, no. 1, pp. 3–22, Jan. 1985, doi: 10.1016/0735-1933(85)90003-X.

[77] “Fundamentals of Heat and Mass Transfer, 8th Edition | Wiley,” Wiley.com. Accessed: Apr. 28, 2025. [Online]. Available: https://www.wiley.com/en-us/Fundamentals+of+Heat+and+Mass+Transfer%2C+8th+Edition-p-9781119353881

[78] M. M. Shah, “Improved correlation for heat transfer during condensation in conventional and mini/micro channels,” *International Journal of Refrigeration*, vol. 98, pp. 222–237, Feb. 2019, doi: 10.1016/j.ijrefrig.2018.07.037.

[79] D. S. Jung, M. McLinden, R. Radermacher, and D. Didion, “A study of flow boiling heat transfer with refrigerant mixtures,” *International Journal of Heat and Mass Transfer*, vol. 32, no. 9, pp. 1751–1764, Sep. 1989, doi: 10.1016/0017-9310(89)90057-4.

[80] Y. Xu and X. Fang, “A new correlation of two-phase frictional pressure drop for condensing flow in pipes,” *Nuclear Engineering and Design*, vol. 263, pp. 87–96, Oct. 2013, doi: 10.1016/j.nucengdes.2013.04.017.

[81] Y. Xu and X. Fang, “A new correlation of two-phase frictional pressure drop for evaporating flow in pipes,” *International Journal of Refrigeration*, vol. 35, no. 7, pp. 2039–2050, Nov. 2012, doi: 10.1016/j.ijrefrig.2012.06.011.

[82] D. A. Yashar, M. J. Wilson, H. R. Kopke, D. M. Graham, J. C. Chato, and T. A. Newell, “An Investigation of Refrigerant Void Fraction in Horizontal, Microfin Tubes,” *HVAC&R Research*, vol. 7, no. 1, pp. 67–82, Jan. 2001, doi: 10.1080/10789669.2001.10391430.

[83] T. W. Simpson, J. D. Poplinski, P. N. Koch, and J. K. Allen, “Metamodels for Computer-based Engineering Design: Survey and recommendations,” *EWC*, vol. 17, no. 2, pp. 129–150, Jul. 2001, doi: 10.1007/PL00007198.

[84] O. Abdelaziz, Aute ,Vikrant, Azarm ,Shapour, and R. and Radermacher, “Approximation-Assisted Optimization for Novel Compact Heat Exchanger Designs,” *HVAC&R Research*, vol. 16, no. 5, pp. 707–728, Sep. 2010, doi: 10.1080/10789669.2010.10390929.

[85] “Statistics for Spatial Data,” in *Statistics for Spatial Data*, John Wiley & Sons, Ltd, 1993, pp. 1–26. doi: 10.1002/9781119115151.ch1.

[86] L. Piegl and W. Tiller, *The NURBS Book*. in Monographs in Visual Communications. Berlin, Heidelberg: Springer, 1995. doi: 10.1007/978-3-642-97385-7.

[87] V. Gnielinski, “New equations for heat and mass transfer in the turbulent flow in pipes and channels,” *NASA STI/Recon Technical Report A*, vol. 41, pp. 8–16, Jan. 1975.

[88] M. M. Shah, “Unified correlation for heat transfer during boiling in plain mini/micro and conventional channels,” *International Journal of Refrigeration*, vol. 74, pp. 606–626, Feb. 2017, doi: 10.1016/j.ijrefrig.2016.11.023.

[89] “Scopus - Document details - FRICTION-FACTOR EQUATION SPANS ALL FLUID-FLOW REGIMES.” Accessed: Apr. 28, 2025. [Online]. Available: https://www.scopus.com/record/display.uri?eid=2-s2.0-0017769439&origin=inward&txGid=dd6167a92f70d4ddc51320dfda98e7ef

[90] M. I. Ali, M. Sadatomi, and M. Kawaji, “Adiabatic two-phase flow in narrow channels between two flat plates,” *The Canadian Journal of Chemical Engineering*, vol. 71, no. 5, pp. 657–666, 1993, doi: 10.1002/cjce.5450710502.

[91] “Private Communications, 2019.”

[92] M. A. Zaman and S. Wang, “Effects of Refrigerant Drop-In (R32/R410) on the Performance of a Heat Pump System,” 2024.

[93] E. Klein, J. Tancabel, V. Aute, J. Muehlbauer, Y. Hwang, and R. Radermacher, “Retrofit and Experimental Validation of a Packaged Air-Conditioning Unit with a Heat Exchanger Utilizing Shape- and Topology-Optimized Tube Bundles.” Accessed: Jun. 10, 2024. [Online]. Available: https://store.accuristech.com/standards/retrofit-and-experimental-validation-of-a-packaged-air-conditioning-unit-with-a-heat-exchanger-utilizing-shape-and-topology-optimized-tube-bundles?product_id=2904883

[94] V. P. Meruva, J. Tancabel, and V. Aute, “Multi-Objective Optimization of Refrigerant Blends for Supermarket Systems,” presented at the 8th IIR International Conference on Sustainability and the Cold Chain | June 9-11 | Tokyo, Japan, Tokyo, Japan: International Institute of Refrigeration, 2024.

[95] V. P. Meruva, J. Tancabel, and V. Aute, “Design Optimization of Heat Exchangers utilizing Shape-Optimized, Non- Round Tubes for a Residential Air-Conditioning System using R290,” presented at the 16th IIR-Gustav Lorentzen Conference on Natural Refrigerants, College Park, MD, USA: International Institute of Refrigeration, 2024.